



HAL
open science

2'3'-cGAMP triggers a STING- and NF- κ B-dependent broad antiviral response in *Drosophila*

Hua Cai, Andreas Holleufer, Bine Simonsen, Juliette Schneider, Aurélie Lemoine, Hans Henrik Gad, Jingxian Huang, Jieqing Huang, Di Chen, Tao Peng, et al.

► **To cite this version:**

Hua Cai, Andreas Holleufer, Bine Simonsen, Juliette Schneider, Aurélie Lemoine, et al.. 2'3'-cGAMP triggers a STING- and NF- κ B-dependent broad antiviral response in *Drosophila*. *Science Signaling*, 2020, 13 (660), pp.eabc4537. 10.1126/scisignal.abc4537 . hal-03037007

HAL Id: hal-03037007

<https://hal.science/hal-03037007v1>

Submitted on 2 Dec 2020

HAL is a multi-disciplinary open access archive for the deposit and dissemination of scientific research documents, whether they are published or not. The documents may come from teaching and research institutions in France or abroad, or from public or private research centers.

L'archive ouverte pluridisciplinaire **HAL**, est destinée au dépôt et à la diffusion de documents scientifiques de niveau recherche, publiés ou non, émanant des établissements d'enseignement et de recherche français ou étrangers, des laboratoires publics ou privés.

1 **2'3'-cGAMP triggers a STING and NF- κ B dependent broad antiviral response in**
2 **Drosophila**

3 Hua Cai^{1,2}, Andreas Holleufer³, Bine Simonsen³, Juliette Schneider², Aurélie Lemoine²,
4 Hans Henrik Gad³, Jingxian Huang¹, Jieqing Huang¹, Di Chen¹, Tao Peng¹, João T.
5 Marques^{4,5}, Rune Hartmann^{3,*}, Nelson E. Martins^{2,*} & Jean-Luc Imler^{2,1}

6

7

8 ¹Sino-French Hoffmann Institute, State Key Laboratory of Respiratory Disease, School
9 of Basic Medical Science, Guangzhou Medical University, Guangzhou, 511436, China.

10 ²Université de Strasbourg, CNRS UPR9022, 67084 Strasbourg, France.

11 ³Department of Molecular Biology and Genetics, Aarhus University, 8000 Aarhus C,
12 Denmark

13 ⁴Université de Strasbourg, CNRS UPR9022, INSERM U1257, 67084 Strasbourg,
14 France.

15 ⁵Department of Biochemistry and Immunology, Instituto de Ciências Biológicas,
16 Universidade Federal de Minas Gerais, Belo Horizonte, Minas Gerais, CEP 31270901,
17 Brazil

18

19

20 *Corresponding authors. rh@mbg.au.dk, nmartins@ibmc-cnrs.unistra.fr

21

22

23

24 **Abstract**

25 We previously reported that an orthologue of STING regulates infection by picorna-like
26 viruses in drosophila. In mammals, STING is activated by the cyclic dinucleotide 2'3'-
27 cGAMP produced by cGAS, which acts as a receptor for cytosolic DNA. Here, we show
28 that injection of flies with 2'3'-cGAMP can induce expression of dSTING-regulated
29 genes. Co-injection of 2'3'-cGAMP with a panel of RNA or DNA viruses results in
30 significant reduction of viral replication. This 2'3'-cGAMP-mediated protection is still
31 observed in flies mutant for the genes *Atg7* and *AGO2*, which encode key components
32 of the autophagy and small interfering RNA pathways, respectively. By contrast, it is
33 abrogated in flies mutant for the NF- κ B transcription factor Relish. Analysis of the
34 transcriptome of 2'3'-cGAMP injected flies reveals a complex pattern of response, with
35 early and late induced genes. Our results reveal that dSTING regulates an NF- κ B -
36 dependent antiviral program, which predates the emergence of interferons in
37 vertebrates.

38

39

40

41

42

43

44

45

46

47 INTRODUCTION

48 Insects, like all animals, are plagued by viral infections, which they oppose through
49 their innate immune system. Induced transcription of antiviral genes upon sensing of
50 infection is a common antiviral response observed across kingdoms. In insects,
51 inducible responses contribute to defense against viruses, together with RNA
52 interference (RNAi) and constitutively expressed restriction factors (reviewed in ¹).
53 Apart from RNAi, these mechanisms are still poorly characterized and appear to be
54 largely virus-specific²⁻⁴. Combining genetics and transcriptomic analysis, we previously
55 showed that the evolutionarily conserved factor drosophila Stimulator of Interferon
56 Genes (dSTING) participates together with the kinase IKK β and the NF- κ B
57 transcription factor Relish in a novel pathway controlling infection by the picorna-like
58 viruses Drosophila C virus (DCV) and Cricket Paralysis Virus (CrPV) in the model
59 organism *Drosophila melanogaster*⁵.

60 In mammals, STING is a central component of the mammalian cytosolic DNA sensing
61 pathway, where it acts downstream of the receptor cyclic GMP-AMP synthase (cGAS)⁶.
62 Upon binding DNA, cGAS synthesizes 2'3'-cGAMP, a cyclic dinucleotide (CDN)
63 secondary messenger that binds to and activates STING⁷⁻¹⁴. Bacteria also synthesize
64 CDNs such as c-di-AMP, c-di-GMP and 3'3'-cGAMP, which can be sensed by STING
65 (reviewed in ¹⁵). Upon activation, STING recruits through its C-terminal tail (CTT)
66 region the kinase TBK1, which phosphorylates and activates the transcription factor
67 Interferon Regulatory Factor (IRF) 3 to trigger interferon (IFN) production¹⁶⁻¹⁸. STING
68 can also activate NF- κ B and autophagy independently from its CTT domain in
69 mammalian cells¹⁹⁻²¹.

70 The identification of STING in animals devoid of interferons, such as insects, raises
71 the question of the ancestral function of this molecule. Invertebrate STING lacks the
72 CTT extension, which was shown to be essential for the activation of IRF transcription
73 factors and induction of interferons²². In contrast, the ability of STING to regulate
74 transcription factors of the NF- κ B family^{5,23,24} or autophagy²⁵, seems conserved
75 throughout metazoa. Importantly, these responses are triggered in a CTT-independent
76 manner in mammals¹⁹⁻²¹. Apart from the missing CTT, the global overall structure of
77 STING is well conserved between vertebrates and invertebrates. Accordingly, in vitro
78 studies with STING recombinant proteins from the sea anemone *Nematostella*
79 *vectensis* (Cnidaria), the oyster *Crassostrea gigas* (Mollusks) and the worm *Capitella*
80 *teleta* (Annelids) revealed that they all bind CDNs²⁶. Intriguingly however, binding of
81 CDNs was not observed with recombinant STING produced from several insect
82 species, including drosophila²⁶.

83 The mechanism by which STING exerts its antiviral effect in insects, which could
84 provide important clues on its ancestral function, is still unclear. Here, we identify 2'3'-
85 cGAMP as a potent agonist of dSTING in vivo and show that it triggers a strong Relish-
86 dependent transcriptional response that confers protection against a broad range of
87 RNA and DNA viruses.

88

89 **RESULTS**

90 **A subset of CDNs trigger expression of STING dependent virus regulated genes**

91 To characterize in vivo the dSTING pathway, we used *dSTING^{Rxn}* (RXN) loss of
92 function mutant flies (fig. S1A). Expression of *dSTING* was reduced by 9- to 27-fold in
93 the mutant, as previously described, but was restored to wild type level when a
94 genomic rescue was introduced in the flies (fig. S1B). Basal levels or induction by DCV
95 of three previously described IKK β and dSTING dependent genes (CG13641,
96 CG42825, and CG33926, hereafter referred to as *sting regulated gene (srg)1*, *srg2*
97 and *srg3*, respectively) was significantly reduced in RXN mutant flies compared to
98 *dSTING^{Control}* (WT) or *dSTING^{Rescue}* flies (fig. S1C-E). By contrast, induction of the gene
99 *Hsp26²⁷* by DCV (fig. S1F) or of NF- κ B-dependent antimicrobial peptide genes by
100 *Listeria monocytogenes* (fig. S2) was not affected in the RXN mutant. We noted that
101 *dSTING* expression was still induced by DCV infection in RXN mutant flies, reaching
102 levels close to uninfected wild type three days post infection (dpi, fig. S1B). We
103 hypothesize that a residual level of dSTING protein in the mutant accounts for some
104 remaining activity of the pathway since neither the promoter nor the open reading
105 frame (ORF) of the short form of dSTING are affected by the RXN deletion (fig. S1A).
106 We next analyzed whether the dSTING pathway could be activated by naturally
107 occurring CDNs known to be agonists of STING in other organisms. Injection of c-di-
108 AMP, 3'3'-cGAMP and 2'3'-cGAMP into WT flies led to a dose-dependent increased
109 expression of *dSTING* and *srg1-3* at 6 and 24 hours post injection (hpi) (Fig. 1A-H and
110 fig. S3). Only c-di-GMP did not trigger a response in these experiments (Fig. 1 and fig.
111 S3, S4). These effects were recapitulated in a cellular model (fig. S5). The induction of
112 *srg1-3* by CDNs was reduced in RXN mutant flies at 6 hpi or abolished at 24 hpi (Fig.
5

113 1B-D and F-H). For *dSTING* itself, the pattern of induction was similar in RXN and WT
114 flies, although the level of expression was always substantially reduced in mutant flies
115 (Fig. 1A,E). Induction of *dSTING* and *srg1* was completely abolished in *dSTING* null
116 mutant flies independently generated using CRISPR (*dSTING*^{L76GfsTer11}) (fig. S6A,B).
117 Finally, induction of *dSTING* and *srg1-3* after 2'3'-cGAMP injection was restored in
118 *dSTING*^{Rescue} flies (fig. S6C-F).

119 Induction of *srg1* and *srg2* by 2'3'-cGAMP was rapid, peaking at 3 or 6 hpi and
120 decreasing afterwards (Fig. 1I,J). Interestingly, inducible expression of *srg3* remained
121 high at 24 hpi (Fig. 1K). Induction of *dSTING* and *srg1-3* by 2'3'-cGAMP was reduced
122 or abolished in *Relish* null mutant flies (Fig. 1L-O), even though the basal level of
123 *dSTING* was not altered (Fig. 1L). Overall, these data reveal that a subset of naturally
124 occurring CDNs can trigger gene expression in *Drosophila*, in a manner dependent on
125 dSTING and Relish.

126

127 **2'3'-cGAMP has a significant impact on the transcriptome of whole flies**

128 Next, we performed genome-wide transcriptomic analysis to identify 2'3'-cGAMP
129 regulated genes in whole flies. We identified 427 stimulated and 545 repressed genes,
130 displaying at least 1.5-fold change in animals injected with 2'3'-cGAMP compared to
131 Tris buffer (Fig. 2A), with 269, 88 and 115 transcripts stimulated and 311, 53 and 63
132 transcripts repressed at the 6, 12 and 24h timepoints, respectively (fig. S7). In contrast,
133 only four stimulated and one repressed transcripts were observed when c-di-GMP was
134 injected into WT flies (Data File S1). Clustering analysis revealed three broad
135 categories of stimulated and repressed genes based on their early, sustained or late
136 kinetics of induction or repression (Fig.2B, Data File S2). Among stimulated genes,

137 *srg1* was induced rapidly, while *srg3* classifies as a late induced gene, confirming our
138 initial observation. Rapidly induced genes included antimicrobial peptides, cytokines
139 such as *spaetzle* and *upd3*, transcription factors (e.g. *Rel*, *kay*, *Ets21C*, *FoxK*) and
140 other signaling molecules (*Tak11*, *pirk*, *Charon*, *dSTING*) (Fig.2C). One of the three
141 canonical components of the siRNA pathway, *AGO2*, was rapidly induced by 2'3'-
142 cGAMP, together with *pst* and *ref(2)P*, which encode restriction factors against
143 picorna-like viruses^{28,29} and rhabdoviruses³⁰, respectively. Late induced genes were
144 mainly unknown but included the JAK-STAT regulated gene *vir-1* and the antiviral gene
145 *Nazo* (Fig. 2C)^{5,31}. Gene ontology analysis revealed that the early and sustained
146 stimulated genes were significantly enriched for genes involved in immunity (Fig. 2D).
147 No such enrichment was detected in the late induced genes. By contrast, the 2'3'-
148 cGAMP repressed genes were associated with mitochondria or belonged to several
149 metabolic pathways, including carbohydrate, lipid and protein metabolism (Fig. 2D).
150 This points to an impact of CDN injection on metabolism, possibly reflecting cellular
151 reprogramming.

152 Then, we performed in silico analysis of predicted binding sites for transcription factors
153 in the stimulated genes. We found that 75% of the stimulated genes (321) contained
154 binding sites for members of the NF- κ B family. While 84% of early and 80% of the
155 sustained genes contained NF- κ B binding sites, only 57% (63) of the late genes
156 contained such binding sites, suggesting a distinct secondary response at 24h post-
157 cGAMP injection. We further analyzed a subset of genes and confirmed that they were
158 induced by 2'3'-cGAMP but not c-di-GMP, and that this induction was dependent on
159 the NF- κ B transcription factor Relish (fig. S8).

160 We could find enrichment for binding sites for other transcription factors that were
161 stimulated by 2'3'-cGAMP, or for transcription factors regulated by induced cytokines
162 (e.g. upd3) (Fig. 2E). Among these, STAT appears to play an important role in all
163 temporal expression profiles, with binding sites in 22%, 42% and 8% of the genes in
164 the early, sustained and late categories, respectively. Others, such as Ets21c, E2F1
165 and AP1 may participate in the early phase of the response to 2'3'-cGAMP, given their
166 enrichment only in the early and sustained stimulated genes (Fig. 2E).

167

168 **Injection of 2'3'-cGAMP protects flies against viral infections**

169 We next addressed the functional consequences of activation of the dSTING pathway
170 by CDN injection. Co-injection of 2'3'-cGAMP with DCV or the related cricket paralysis
171 virus (CrPV) resulted in a significant decrease of viral RNA accumulation in WT flies
172 (Fig. 3A-B). Such a protective effect of 2'3'-cGAMP was not observed in RXN mutant
173 flies, but was restored in *dSTING^{Rescue}* flies (fig. S9), indicating that it was dependent
174 on dSTING. Accordingly, 2'3'-cGAMP improved the survival of DCV infected WT flies
175 but not of RXN mutants (Fig. 3C). Co-injection of 2'3'-cGAMP but not c-di-GMP also
176 resulted in reduced accumulation of viral RNA for three other viruses, namely the
177 positive strand RNA virus Flock house virus (FHV), the negative strand RNA virus
178 vesicular stomatitis virus (VSV), and the double strand DNA virus Kallithea virus (KV)
179 (Fig. 3D-F). Collectively, these results indicate that 2'3'-cGAMP triggers protection
180 against a broad range of viruses.

181

182 **2'3'-cGAMP acts independently of the siRNA response and autophagy, but**
183 **depends upon the NF- κ B transcription factor Relish for its antiviral role**

184 To identify the mechanism by which 2'3'-cGAMP exerts its antiviral activity, we first
185 analyzed the effect of CDNs on DCV and VSV infection in *AGO2* null mutant flies. We
186 observed a reduced accumulation of viral RNAs when 2'3'-cGAMP was co-injected
187 with the viruses in both mutant and control flies, revealing that the antiviral function of
188 the CDN does not depend on this key component of the antiviral siRNA pathway (Fig.
189 4A,B). Similarly, 2'3'-cGAMP substantially reduced viral RNA accumulation in *Atg7*
190 null mutant flies, ruling out an involvement of the canonical autophagy pathway (Fig.
191 4C). By contrast, the protective effect of 2'3'-cGAMP against DCV, CrPV and VSV was
192 completely abolished in *Relish* mutant flies (Fig. 4D-F). Altogether, these results reveal
193 that 2'3'-cGAMP triggers a dSTING-NF- κ B-dependent antiviral transcriptional
194 response, independent from RNA interference or autophagy.
195

196 **DISCUSSION**

197 **CDNs activate antiviral immunity in *Drosophila***

198 Our results reveal that three out of the four naturally occurring CDNs that activate
199 mammalian STING can also trigger the dSTING signaling pathway in flies. They raise
200 the question of the mechanism by which 2'3'-cGAMP activates dSTING. Like others²⁶,
201 we have not been able to detect binding of 2'3'-cGAMP to purified recombinant
202 dSTING. Native purification of the dSTING ligand binding domain expressed in *E. coli*
203 or denaturative purification from *E. coli* inclusion bodies followed by in vitro refolding,
204 resulted in aggregation-prone unstable proteins. This suggested us that the purified
205 protein was not folding correctly. By contrast, we had no difficulties in purifying various
206 mammalian versions of STING using published protocols. The recently reported
207 cryoEM structure of full length chicken STING reveals substantial interaction of the
208 ligand binding domain with areas of the transmembrane domains at the N-terminus of
209 the protein³². We believe that such interaction may be critical for either ligand binding
210 or stability (or both) of the cytosolic domain of dSTING, a hypothesis supported by the
211 sequence divergence between the transmembrane domains of STING in mammals
212 and drosophila.

213 Our work complements the molecular study of Kranzusch and colleagues, who
214 reported binding of CDNs to STING from the sea anemone *N. vectensis*, and supports
215 the hypothesis that the ancestral function of STING in metazoans was to sense CDNs²⁶.
216 Bacteria produce a diversity of CDNs and cyclic trinucleotides, some of which could
217 activate dSTING^{23,33}. Martin *et al* reported that c-di-GMP was able to activate a
218 dSTING-dependent response to *Listeria monocytogenes* infection²³. However, we did
219 not observe an effect of c-di-GMP upon injection into flies or a contribution of dSTING

220 to induction of antimicrobial peptides following infection by *L. monocytogenes*. Further
221 experiments comparing mutant alleles and taking other parameters (e.g. microbiota)
222 into consideration are required to clarify the differences between the two studies.
223 Of note, bacterial CDNs have two canonical 3',5' phosphodiester-linkages, whereas
224 mammalian and *Nematostella* cGAS produce chemically distinct CDNs containing one
225 2',5' phosphodiester bond joining G to A and one canonical 3',5'- phosphodiester bond
226 joining A to G^{21,26}. While we detected activity of 3'3'-CDNs, namely of 3'3'-cGAMP and
227 of c-di-AMP, the strongest agonist was 2',3'-cGAMP, suggesting that an enzyme
228 producing this CDN exists in insects. Indeed, Wang and colleagues recently reported
229 the inducible production of cGAMP in the cytosol of *Bombyx mori* cells infected with
230 nucleopolyhedrovirus (NPV)²⁴. Thus, the production of CDNs in the response to virus
231 infection appears to be ancient, possibly inherited in early eukaryotes from
232 prokaryotes^{22,34}. A major goal for future study will be the identification and
233 characterization of the cGAS enzyme operating in *Drosophila*.

234

235 **Activation of NF- κ B is an ancestral function of the dSTING pathway**

236 One major difference between STING in mammals and invertebrates, e.g.
237 *Nematostella* and *Drosophila*, is the lack of the CTT domain that mediates interaction
238 with and activation of the kinase TBK1 and the IRF3 transcription factor²². This has led
239 to the hypothesis that invertebrate STING regulates autophagy rather than a
240 transcriptional response. Indeed, STING activates autophagy through a mechanism
241 independent of TBK1 activation and IFN induction in mammals. Furthermore,
242 NvSTING also induces autophagy when it is ectopically expressed in human cells²¹. In
243 *Drosophila*, autophagy was found to participate in the control of some viruses, but not

244 others and the effect was modest compared to RNA interference^{35,36}. Recently,
245 dSTING-dependent autophagy has been proposed to restrict Zika virus infection in the
246 brain, although autophagy constituents are proviral for Zika and other flaviviruses in
247 mammalian cells^{25,37}. Our results using *ATG7* mutant flies indicate that 2'3'-cGAMP
248 can control viral infection independently from the canonical autophagy pathway, but
249 requires both dSTING and Relish. However, we cannot rule out a virus-specific (e.g.
250 Zika virus) role and the involvement of an unconventional autophagy pathway. Indeed,
251 LC3 lipidation in response to cGAMP stimulation in human cells does not depend on
252 the ULK kinases or Beclin 1, two essential components of the classical autophagy
253 pathway²¹. In this regard, we note that one of the genes stimulated by cGAMP is *ref(2)P*,
254 the ortholog of the autophagy receptor p62 and a restriction factor for Sigma virus³⁰.
255 Even though we cannot completely rule out a contribution of autophagy, our results
256 point to the central role played by the NF- κ B transcription factor Relish in the antiviral
257 response triggered by 2'3'-cGAMP. Further analysis will be required to precisely define
258 the contribution of Relish in this response. The dSTING-dependent transcriptional
259 response to cGAMP injection is complex, involving stimulation and repression of gene
260 expression occurring in different waves, with early and late responses. However, the
261 presence of consensus binding sites for NF- κ B in the *cis*-regulatory regions of ~75%
262 of the stimulated genes, regardless of their kinetics of induction, confirms a major
263 contribution of Relish. In addition, we identified 13 other transcription factors and 2
264 cytokines (*upd3* and *spz*) in the early and sustained stimulated genes (Data File S3).
265 Among the stimulated transcription factors, *kay* (the *Drosophila* ortholog of c-Fos),
266 *Ets21C* and *FoxK* were previously implicated in immune, inflammatory or stress
267 responses in *Drosophila*³⁸⁻⁴⁰. The *cis*-regulatory regions of the differentially expressed
12

268 genes were enriched for binding sites for the mentioned transcription factors and
269 STAT92E, the sole *Drosophila* STAT ortholog (Fig. 3D, Data File S4). These different
270 transcriptional regulators may coordinate the kinetics of the response and induction of
271 different sets of genes in the context of bacteria and virus infection.

272

273 **A broad antiviral induced response in *Drosophila***

274 We observed a striking antiviral activity of 2'3'-cGAMP against a broad range of viruses
275 with DNA or RNA genomes. This contrasts with previous studies that reported virus-
276 specific induced responses^{2,41-45}, leading to the idea that RNA interference is the only
277 pathway acting on the broad range of viruses infecting invertebrates, which are devoid
278 of interferons. In this regard, we showed that the antiviral effect of 2'3'-cGAMP does
279 not require AGO2, a key component of the antiviral RNAi pathway in flies, even though
280 this gene is stimulated by the CDN. Thus, besides RNAi, an induced antiviral response
281 involving dSTING contributes to host defense against a range of viruses in *Drosophila*.
282 Furthermore, the induction of AGO2 by CDNs suggest a crosstalk between the two
283 pathways where activation of dSTING may potentiate the siRNA response. Intriguingly,
284 while our data are consistent with 2'3'-cGAMP triggering dSTING-dependent antiviral
285 immunity, it is less clear that viral infection in flies is capable of inducing CDN
286 production and STING-dependent responses. In particular, we did not observe
287 increased DCV replication in *dSTING* and *Relish* mutant flies, in contrast to what we
288 previously reported⁵. The reason for this discrepancy is not clear at present, but may
289 involve changes in the microbiota of the flies. Indeed, we note that several of the
290 dSTING- and IKK β -dependent genes that we identified can be regulated by the
291 microbiota⁴⁶. Our previous results pointed to a specific contribution of the dSTING-

292 IKK β -Relish pathway in resistance to DCV and CrPV, although a significant but smaller
293 effect was visible also for VSV⁵. This apparent discrepancy could be explained by
294 differences between viruses in the induction of the pathway based on their tissue
295 tropisms, the type of virus-associated molecular pattern produced or the existence of
296 escape strategies, all of which may be bypassed by systemic injection of 2'3'-cGAMP.
297 A number of previous studies reported strong transcriptional responses to virus
298 infection in insects^{2,27,31,43,47,48}, but also *C. elegans*⁴⁹, oysters⁵⁰ and shrimps⁵¹. Analysis
299 of the transcriptional response to viral infections in vivo is complicated by the fact that
300 (i) cell infections are unsynchronized; (ii) host cells are modified through hijacking of
301 cellular functions by viruses; and (iii) many viruses trigger cell lysis and tissue damage,
302 making it complicated to discern the immune response from the non-specific response
303 to stress. Consequently, the transcriptome of virus-infected flies only provides a blurred
304 image of the induced antiviral response^{2,27,31,43,44,48}. Identification of an agonist of
305 dSTING bypasses the need for the use of viruses and provides a much clearer picture
306 of the modifications of the drosophila transcriptome associated with induction of
307 antiviral immunity. In particular, our data suggest that 2'3'-cGAMP triggers the
308 expression of cytokines (e.g. Spaetzle, upd3) that amplify the response and trigger
309 expression of antiviral effectors (e.g. Nazo, vir-1). The tools are now at hands to
310 characterize the induced mechanisms controlling viruses in insects, which may reveal
311 original targets for antiviral therapy.

312

313 **Materials and Methods**

314 **Drosophila strains**

315 Fly stocks were raised on standard cornmeal agar medium at 25°C. All fly lines used
316 in this study were *Wolbachia* free. *w*¹¹¹⁸, *dSTING*^{Control}, *dSTING*^{Rxn}, *yellow (y) white*
317 (*w*) *DD1*, *yw;AGO2*⁴¹⁴, *Atg7*^{d14}/*Cyo-GFP*, *Atg7*^{d77}/*Cyo-GFP* and *CG5335*^{d30}/*Cyo-GFP*
318 stocks have been described previously⁵². *Relish*^{E20} flies isogenized to the DrosDel
319 *w*¹¹¹⁸ isogenic background were a gift from Dr. Luis Teixeira (Instituto Gulbenkian de
320 Ciência)⁴⁵.

321 *dSTING*^{L76GfsTer11} mutants were generated by CRISPR/Cas mediated mutagenesis in
322 a *yw* mutant background. The four base-pairs deletion was verified by Sanger
323 sequencing (Eurofins Genomics), using the sequencing primers described in table S5.

324 Crossing schemes and detailed injection protocols are available upon request.

325 The genomic rescue of wild-type *dSTING* was established by PhiC31 mediated
326 transgenesis. The fosmid FlyFos015653⁵³ was injected into the *y*¹ *w*¹¹¹⁸; *PBac{y[+]-*
327 *attP-9A}VK00027* (BDSC#9744) line and introgressed into a *dSTING*^{Rxn} mutant
328 background by standard genetic crossing techniques. Transgenesis and initial
329 recombinant fly selection was done by the company BestGene.

330

331 **Virus infection**

332 Viral stocks were prepared in 10 mM Tris-HCl, pH 7.5. Infections were performed with
333 3–5 days old adult flies by intrathoracic injection (Nanoject II apparatus, Drummond
334 Scientific) with 4.6 nL of DCV solution (500 PFU/fly). Injection of the same volume of
335 10 mM Tris-HCl, pH 7.5, was used as a negative control.

336

337 **Bacterial infections**

338 *Listeria monocytogenes* (strain 10403S) cultures were grown in brain heart infusion
339 (BHI) medium at 28°C. Infections were performed with 3-5 days old adult flies by
340 intrathoracic injection (Nanoject II apparatus) with 9.2 nL of *L. monocytogenes* solution
341 in PBS (OD600=0.001). The dose used was determined by titration, comparing the
342 wild-type strain to its listeriolysin O-deletion mutant (*L. monocytogenes* Δ hly, a kind gift
343 of P. Cossart) to ensure that the response to cytosolic *L. monocytogenes* was
344 monitored⁵⁴. Injection of the same volume of PBS was used as a negative control.
345 Injected flies were kept at 28°C and collected in pools of 6 individuals (3 males + 3
346 females) at the indicated time points for RNA extraction and RT-qPCR.

347

348 **CDNs injection with or without viruses**

349 The CDNs (Invivogen) were dissolved in 10 mM Tris pH 7.5 to a concentration of 0.9
350 mg/mL, and their integrity was monitored by chromatography, as described⁵⁵. 3–5 days
351 old adult flies were CDN stimulated. For CDN injection, each fly was injected with 69
352 nL of CDN solution or 10 mM Tris pH 7.5 (negative control) by intrathoracic injection
353 using a Nanoject II apparatus. For CDNs and virus coinjection, 30 μ L 0.9 mg/mL CDNs
354 were mixed with 2 μ L virus (DCV 5PFU/4.6 nL, CRPV 5PFU/4.6 nL, VSV 5000PFU/4.6
355 nL, FHV 500PFU/4.6 nL and KV). Each fly was injected with 69 nL of CDNs or 10 mM
356 Tris pH 7.5 plus virus mixture by intrathoracic injection using a Nanoject II apparatus
357 (Drummond Scientific) and injected flies were collected in pools of 6 individuals (3
358 males + 3 females) at indicated time points and homogenized for RNA extraction and
359 RT-qPCR.

360

361 **CDN transfection of drosophila S2 cells**

362 *Drosophila* Schneider 2 (S2) cells were seeded in 12 well plates (2×10^6 cells per well)
363 in Schneider's Insect Medium (Sigma-Aldrich) supplemented with 10 % fetal bovine
364 serum (FBS) (Sigma-Aldrich), 100 U/ml penicillin (Sigma-Aldrich) and 100 μ g/ml
365 streptomycin (Sigma-Aldrich). 3 h later, the cells were transfected with 10 μ g CDN per
366 well using 2 μ l Lipofectamine 2000 (ThermoFisher Scientific) according to the
367 manufacturer's protocol. Unsupplemented Schneider's Insect Medium was used for
368 making the transfection complexes. After 6 or 24 hours of transfection, cells were
369 harvested for RNA extraction and qRT-PCR.

370

371 **RNA extraction and qRT-PCR of *D. melanogaster* tissues**

372 Total RNA from collected flies was extracted using a Trizol Reagent RT bromoanisole
373 solution (MRC), according to the manufacturer's instructions. 1 μ g total RNA was
374 reverse transcribed using an iScript™ gDNA clear cDNA synthesis Kit (Biorad),
375 according to the manufacturer's instructions. The DNase and RNA reaction mixture
376 was incubated for 5 min at 25°C to remove genomic DNA and then the reaction was
377 stopped by heating at 75°C for 5min. Then reverse transcription mix was added to
378 DNase-treated RNA template and cDNA was synthesized in the following PCR
379 program: 1) 25°C, 5 min; 2) 46°C, 20 min; 3) 95°C, 1 min. cDNA was used for
380 quantitative real time PCR (qRT-PCR), using iQ™ Custom SYBR Green Supermix Kit
381 (Biorad) according to the manufacturer's instructions and the following qPCR program:
382 1) 98°C, 15 s; 2) 95°C, 2 s; 3) 60°C, 30 s; 4) plate read; 5) go to step 2, 34X on a
383 CFX384 Touch™ Real-Time PCR platform (Bio-Rad). Primers used for qRT-PCR are
384 listed in table S1. Normalization was performed relative to the housekeeping gene
385 *RpL32*.

386

387 **RNA extraction and qRT-PCR of drosophila S2 cells**

388 Total RNA was extracted using the EZNA Total RNA Kit I (Omega Bio-tek) following
389 the manufacturer's protocol. cDNA was generated with random hexamer primers and
390 the RevertAid RT Reverse Transcription Kit (ThermoFisher Scientific) using 1 µg total
391 RNA as template, following the manufacturer's protocol. cDNA was diluted five times
392 and used as templates for qRT-PCR on a LightCycler® 480 Instrument II (Roche) using
393 LightCycler® 480 SYBR Green I Master reaction mix (Roche) according to the
394 manufacturer's instructions and the following qPCR program: 1) 95°C, 5 min; 2) 95°C,
395 10 s; 3) 55°C; 10 s; 4) 72°C, 10 s; 5) plate read; 6) go to step 2, 44X. Primers used for
396 qRT-PCR are listed in table S1. Normalization was performed relative to the
397 housekeeping gene *RpL32*.

398

399 **RNA-Sequencing of *D. melanogaster* injected with CDNs**

400 Male flies of *dSTING*^{Control} were injected with 69 nL/fly of either 10 mM Tris (pH 7.5), c-
401 di-GMP (1mg/mL) or 2,3-cGAMP (1 mg/mL) by intrathoracic injection (Nanoject II
402 apparatus), in three independent experiments. Injected flies were collected in pools of
403 6 individuals at 6-, 12- and 24-hours post injection. Total RNA was isolated from
404 injected flies using TRIzol™ Reagent (Invitrogen), according to the manufacturer's
405 protocol. RNA quantity and purity were assessed using a Dw-K5500
406 spectrophotometer (Drawell) and Agilent 2200 TapeStation (Agilent). rRNA was
407 removed using Epicentre Ribo-Zero rRNA Removal Kit (Illumina), and RNA was
408 converted to cDNA. Prepared cDNA was used for Illumina sequencing library
409 preparation using NEBNext® Ultra™ Directional RNA Library Prep Kit for Illumina
18

410 (NEB), following the manufacturer's instructions. Briefly, DNA fragments were end
411 repaired to generate blunt ends with 5'phosphatase and 3'hydroxyls, before adapters
412 ligation, PCR amplification and cleanup. Average fragment length was 300-bp. Purity
413 of the libraries was evaluated using an Agilent 2200 TapeStation. Libraries were used
414 for cluster generation in situ on an HiSeq paired-end flow cell using the Rapid mode
415 cluster generation system, followed by massively parallel sequencing (2×150 bp) on
416 an HiSeq X Ten. Library construction, high throughput sequencing, adapter removal
417 and initial quality control and trimming were done by the company Ribobio.

418

419 **Transcriptome analysis**

420 After quality trimming and adapter removal using Trimmomatic, reads were mapped
421 using STAR v2.5.3⁵⁶ to the Drosophila genome and annotation (ENSEMBL BDGP6.22).
422 Reads mapping to the sense strand of the transcripts were counted with featureCounts
423 v1.6.2⁵⁷, using the Drosophila annotation files, allowing mapping to multiple genes.
424 Differential gene expression of transcripts present in ≥20% of the libraries with at least
425 5 reads across all libraries was done using the *deseq* function of the "DESeq2" (v1.20)
426 package⁵⁸. Variance was estimated using the local fitting method. Read counts and
427 normalized read counts are shown in GEO dataset GSE140955. Transcripts with log2
428 difference in expression ≥ 1.5 and Benjamini & Hochberg corrected P-value < 0.05
429 were considered differentially expressed.

430

431 **Clustering of temporal expression profiles**

432 All differentially expressed genes between Tris and 2'3'-cGAMP injected WT flies at
433 any time point or on average across all time points were clustered in temporal

434 expression categories by partitioning around medoids (PAM) clustering using the *pam*
435 function in the “cluster” (v2.1.0) package. The optimal number of clusters for either
436 stimulated or repressed genes was determined using the gap statistic method, as
437 implemented in the *fviz_nbclust* function of the “factoextra” (v1.0.5) package, using
438 default parameters (100 bootstrapped replications, 10 maximum allowed clusters).
439 Gene expression clusters were visualized using the *Heatmap* function of the
440 “ComplexHeatmap” (v2.0.0) package and *ggplot* of the “ggplot2” (v3.2.1) package.

441

442 **Ontology analysis**

443 Differentially expressed genes between Tris and 2’3’-cGAMP injected WT flies in each
444 temporal expression category were tested for enrichment relative to all genes passing
445 the expression cutoff in any gene ontology type (Molecular Function, Cellular
446 Compartment, Biological Process), using the “Generic GO subset” of gene ontology
447 terms (downloaded from <http://current.geneontology.org/ontology/subsets/index.html>
448 on 10/10/2019). Gene ontology enrichment analysis was done using the *enricher*
449 function of “clusterProfiler” package (v3.1.12), using default parameters (Benjamini &
450 Hochberg corrected P-value cutoff of 0.05).

451

452 **Transcription Factor Enrichment Analysis**

453 Enrichment of transcription factor binding sites (TFBS) in the regulatory regions of the
454 differentially expressed genes was done using the *cisTarget* function of the “RcisTarget”
455 package (v1.4.0)⁵⁹. The database “dm6-5kb-upstream-full-tx-11species.mc8nr”
456 database was used, which includes the rankings for conserved TFBS in the non-coding
457 regions 5 kb upstream of the transcription start site and in introns of all annotated

458 genes in the *D. melanogaster* genome (r6.02). Gene symbols were updated to the
459 r6.04 annotation when necessary. Transcription factor family assignment was done
460 according to Flybase (FB2019_05).

461

462 **Statistical analysis**

463 For quantification of viral RNA loads and target gene expression, log transformed ratios
464 were compared using linear regression models using the *lm* function of base R.
465 Survival curves were analysed by Cox regression using the *coxph* function in the
466 “survival” (v2.44-1.1) package. Depending on the experiment, independent variables
467 included genotype, virus injection, CDN injection and time post injection and all
468 interactions between them. Experiment was included as an independent variable in all
469 tests, and the values for each point are shown normalized by adding/subtracting the
470 mean difference between its respective experiment to the grand mean of all log ratios.
471 Multiple comparisons between the groups of interest were done using the *emmeans*
472 function of the “emmeans” (v1.4.1) package, using Dunnett’s (for control vs treatment
473 comparisons) or Holm’s P value correction. Data were analysed using R (v3.4.2) and
474 *ggplot* was used for plotting.

475

476 **Supplementary Materials**

477 **Figure S1** – DCV infection induces a dSTING dependent transcriptional response in
478 *D. melanogaster*.

479

480 **Figure S2** – Antimicrobial peptide gene induction is not affected in *dSTING* mutant
481 flies after *L. monocytogenes* challenge.

482

483 **Figure S3** – The cyclic dinucleotides 2'3'-cGAMP, 3'3'-cGAMP and c-di-AMP have a
484 dose dependent effect on the expression of a *dSTING* regulated gene.

485

486 **Figure S4** – c-di-GMP injection does not induce antimicrobial peptide expression.

487

488 **Figure S5** – The cyclic dinucleotides 2'3'-cGAMP and 3'3'-cGAMP induce *dSTING*
489 dependent genes in a cellular model.

490

491 **Figure S6** – Induction of gene expression following 2'3'-cGAMP injection depends on
492 *dSTING*.

493

494 **Figure S7** – Differentially expressed transcripts between Tris and 2'3'-cGAMP injected
495 flies in the different timepoints.

496

497 **Figure S8** – 2'3'-cGAMP induced gene expression is *Relish* dependent.

498

499 **Figure S9** – A *dSTING* rescue transgene restores 2'3'-cGAMP induced antiviral
500 protection.

501

502 **Table S1** – List of used oligonucleotide primers.

503

504 **Data S1** – Differentially expressed genes between Tris and c-di-GMP injected
505 *dSTING*^{Control} flies at 6, 12 and 24 hours post-injection.

506

507 **Data S2** – Differentially expressed genes between Tris and 2'3'-cGAMP injected
508 *dSTING*^{Control} flies at 6, 12 and 24 hours post-injection.

509

510 **Data S3** – Differentially expressed transcription factors or cytokines between Tris and
511 2'3'-cGAMP injected *dSTING*^{Control} flies at 6, 12 and 24 hours post-injection.

512

513 **Data S4** – Presence of binding sites for stimulated transcription factors in differentially
514 expressed genes.

515

516 **References:**

- 517 1 Mussabekova, A., Daeffler, L. & Imler, J. L. Innate and intrinsic antiviral
518 immunity in *Drosophila*. *Cellular and molecular life sciences : CMLS* **74**, 2039-
519 2054, doi:10.1007/s00018-017-2453-9 (2017).
- 520 2 Kemp, C. *et al.* Broad RNA interference-mediated antiviral immunity and virus-
521 specific inducible responses in *Drosophila*. *Journal of immunology* **190**, 650-
522 658, doi:10.4049/jimmunol.1102486 (2013).
- 523 3 Cao, C., Cogni, R., Barbier, V. & Jiggins, F. M. Complex Coding and Regulatory
524 Polymorphisms in a Restriction Factor Determine the Susceptibility of
525 *Drosophila* to Viral Infection. *Genetics* **206**, 2159-2173,
526 doi:10.1534/genetics.117.201970 (2017).
- 527 4 Cao, C., Magwire, M. M., Bayer, F. & Jiggins, F. M. A Polymorphism in the
528 Processing Body Component Ge-1 Controls Resistance to a Naturally
529 Occurring Rhabdovirus in *Drosophila*. *PLoS Pathog* **12**, e1005387,
530 doi:10.1371/journal.ppat.1005387 (2016).
- 531 5 Goto, A. *et al.* The Kinase IKKbeta Regulates a STING- and NF-kappaB-
532 Dependent Antiviral Response Pathway in *Drosophila*. *Immunity* **49**, 225-234
533 e224, doi:10.1016/j.immuni.2018.07.013 (2018).
- 534 6 Sun, L. J., Wu, J. X., Du, F. H., Chen, X. & Chen, Z. J. J. Cyclic GMP-AMP
535 Synthase Is a Cytosolic DNA Sensor That Activates the Type I Interferon
536 Pathway. *Science* **339**, 786-791, doi:10.1126/science.1232458 (2013).
- 537 7 Wu, J. X. *et al.* Cyclic GMP-AMP Is an Endogenous Second Messenger in
538 Innate Immune Signaling by Cytosolic DNA. *Science* **339**, 826-830,
539 doi:10.1126/science.1229963 (2013).

- 540 8 Gao, D. *et al.* Cyclic GMP-AMP synthase is an innate immune sensor of HIV
541 and other retroviruses. *Science* **341**, 903-906, doi:10.1126/science.1240933
542 (2013).
- 543 9 Ablasser, A. *et al.* cGAS produces a 2'-5'-linked cyclic dinucleotide second
544 messenger that activates STING. *Nature* **498**, 380-384,
545 doi:10.1038/nature12306 (2013).
- 546 10 Diner, E. J. *et al.* The innate immune DNA sensor cGAS produces a
547 noncanonical cyclic dinucleotide that activates human STING. *Cell Rep* **3**, 1355-
548 1361, doi:10.1016/j.celrep.2013.05.009 (2013).
- 549 11 Zhang, X. *et al.* Cyclic GMP-AMP containing mixed phosphodiester linkages is
550 an endogenous high-affinity ligand for STING. *Mol Cell* **51**, 226-235,
551 doi:10.1016/j.molcel.2013.05.022 (2013).
- 552 12 Civril, F. *et al.* Structural mechanism of cytosolic DNA sensing by cGAS. *Nature*
553 **498**, 332-337, doi:10.1038/nature12305 (2013).
- 554 13 Kranzusch, P. J., Lee, A. S., Berger, J. M. & Doudna, J. A. Structure of human
555 cGAS reveals a conserved family of second-messenger enzymes in innate
556 immunity. *Cell Rep* **3**, 1362-1368, doi:10.1016/j.celrep.2013.05.008 (2013).
- 557 14 Gao, P. *et al.* Cyclic [G(2',5')pA(3',5')p] is the metazoan second messenger
558 produced by DNA-activated cyclic GMP-AMP synthase. *Cell* **153**, 1094-1107,
559 doi:10.1016/j.cell.2013.04.046 (2013).
- 560 15 Kranzusch, P. J. cGAS and CD-NTase enzymes: structure, mechanism, and
561 evolution. *Curr Opin Struct Biol* **59**, 178-187, doi:10.1016/j.sbi.2019.08.003
562 (2019).
- 563 16 Motwani, M., Pesiridis, S. & Fitzgerald, K. A. DNA sensing by the cGAS-STING
564 pathway in health and disease. *Nat Rev Genet* **20**, 657-674,
565 doi:10.1038/s41576-019-0151-1 (2019).
- 566 17 Zhang, C. *et al.* Structural basis of STING binding with and phosphorylation by
567 TBK1. *Nature* **567**, 394-398, doi:10.1038/s41586-019-1000-2 (2019).
- 568 18 Liu, S. *et al.* Phosphorylation of innate immune adaptor proteins MAVS, STING,
569 and TRIF induces IRF3 activation. *Science* **347**, aaa2630,
570 doi:10.1126/science.aaa2630 (2015).
- 571 19 Cerboni, S. *et al.* Intrinsic antiproliferative activity of the innate sensor STING in
572 T lymphocytes. *J Exp Med* **214**, 1769-1785, doi:10.1084/jem.20161674 (2017).
- 573 20 de Oliveira Mann, C. C. *et al.* Modular Architecture of the STING C-Terminal
574 Tail Allows Interferon and NF-kappaB Signaling Adaptation. *Cell Rep* **27**, 1165-
575 1175.e1165, doi:10.1016/j.celrep.2019.03.098 (2019).
- 576 21 Gui, X. *et al.* Autophagy induction via STING trafficking is a primordial function
577 of the cGAS pathway. *Nature* **567**, 262-266, doi:10.1038/s41586-019-1006-9
578 (2019).
- 579 22 Margolis, S. R., Wilson, S. C. & Vance, R. E. Evolutionary Origins of cGAS-
580 STING Signaling. *Trends Immunol* **38**, 733-743, doi:10.1016/j.it.2017.03.004
581 (2017).
- 582 23 Martin, M., Hiroyasu, A., Guzman, R. M., Roberts, S. A. & Goodman, A. G.
583 Analysis of *Drosophila* STING Reveals an Evolutionarily Conserved
584 Antimicrobial Function. *Cell Rep* **23**, 3537-3550 e3536,
585 doi:10.1016/j.celrep.2018.05.029 (2018).

- 586 24 Hua, X. *et al.* Stimulator of interferon genes (STING) provides insect antiviral
587 immunity by promoting Dredd caspase-mediated NF-kappaB activation. *The*
588 *Journal of biological chemistry* **293**, 11878-11890,
589 doi:10.1074/jbc.RA117.000194 (2018).
- 590 25 Liu, Y. *et al.* Inflammation-Induced, STING-Dependent Autophagy Restricts
591 Zika Virus Infection in the Drosophila Brain. *Cell host & microbe* **24**, 57-68 e53,
592 doi:10.1016/j.chom.2018.05.022 (2018).
- 593 26 Kranzusch, P. J. *et al.* Ancient Origin of cGAS-STING Reveals Mechanism of
594 Universal 2',3' cGAMP Signaling. *Mol Cell* **59**, 891-903,
595 doi:10.1016/j.molcel.2015.07.022 (2015).
- 596 27 Merklings, S. H. *et al.* The heat shock response restricts virus infection in
597 Drosophila. *Sci Rep* **5**, 12758, doi:10.1038/srep12758 (2015).
- 598 28 Martins, N. E. *et al.* Host adaptation to viruses relies on few genes with different
599 cross-resistance properties. *Proceedings of the National Academy of Sciences*
600 *of the United States of America* **111**, 5938-5943, doi:10.1073/pnas.1400378111
601 (2014).
- 602 29 Magwire, M. M. *et al.* Genome-wide association studies reveal a simple genetic
603 basis of resistance to naturally coevolving viruses in Drosophila melanogaster.
604 *PLoS Genet* **8**, e1003057, doi:10.1371/journal.pgen.1003057 (2012).
- 605 30 Bangham, J., Kim, K. W., Webster, C. L. & Jiggins, F. M. Genetic variation
606 affecting host-parasite interactions: different genes affect different aspects of
607 sigma virus replication and transmission in Drosophila melanogaster. *Genetics*
608 **178**, 2191-2199, doi:10.1534/genetics.107.085449 (2008).
- 609 31 Dostert, C. *et al.* The Jak-STAT signaling pathway is required but not sufficient
610 for the antiviral response of drosophila. *Nature immunology* **6**, 946-953,
611 doi:10.1038/ni1237 (2005).
- 612 32 Shang, G., Zhang, C., Chen, Z. J., Bai, X. C. & Zhang, X. Cryo-EM structures
613 of STING reveal its mechanism of activation by cyclic GMP-AMP. *Nature* **567**,
614 389-393, doi:10.1038/s41586-019-0998-5 (2019).
- 615 33 Whiteley, A. T. *et al.* Bacterial cGAS-like enzymes synthesize diverse nucleotide
616 signals. *Nature* **567**, 194-199, doi:10.1038/s41586-019-0953-5 (2019).
- 617 34 Cohen, D. *et al.* Cyclic GMP-AMP signalling protects bacteria against viral
618 infection. *Nature*, doi:10.1038/s41586-019-1605-5 (2019).
- 619 35 Lamiable, O. *et al.* Analysis of the Contribution of Hemocytes and Autophagy to
620 Drosophila Antiviral Immunity. *J Virol* **90**, 5415-5426, doi:10.1128/JVI.00238-16
621 (2016).
- 622 36 Shelly, S., Lukinova, N., Bambina, S., Berman, A. & Cherry, S. Autophagy is an
623 essential component of Drosophila immunity against vesicular stomatitis virus.
624 *Immunity* **30**, 588-598, doi:10.1016/j.immuni.2009.02.009 (2009).
- 625 37 Abernathy, E. *et al.* Differential and convergent utilization of autophagy
626 components by positive-strand RNA viruses. *PLoS Biol* **17**, e2006926,
627 doi:10.1371/journal.pbio.2006926 (2019).
- 628 38 Myllymaki, H., Valanne, S. & Ramet, M. The Drosophila imd signaling pathway.
629 *Journal of immunology* **192**, 3455-3462, doi:10.4049/jimmunol.1303309 (2014).
- 630 39 Mundorf, J., Donohoe, C. D., McClure, C. D., Southall, T. D. & Uhlirova, M.
631 Ets21c Governs Tissue Renewal, Stress Tolerance, and Aging in the Drosophila

632 Intestine. *Cell Rep* **27**, 3019-3033 e3015, doi:10.1016/j.celrep.2019.05.025
633 (2019).

634 40 Panda, D. *et al.* The transcription factor FoxK participates with Nup98 to
635 regulate antiviral gene expression. *MBio* **6**, doi:10.1128/mBio.02509-14 (2015).

636 41 West, C. *et al.* IIV-6 Inhibits NF-kappaB Responses in Drosophila. *Viruses* **11**,
637 doi:10.3390/v11050409 (2019).

638 42 Panda, D. *et al.* Nup98 promotes antiviral gene expression to restrict RNA viral
639 infection in Drosophila. *Proceedings of the National Academy of Sciences of the*
640 *United States of America* **111**, E3890-3899, doi:10.1073/pnas.1410087111
641 (2014).

642 43 Palmer, W. H., Medd, N. C., Beard, P. M. & Obbard, D. J. Isolation of a natural
643 DNA virus of Drosophila melanogaster, and characterisation of host resistance
644 and immune responses. *PLoS Pathog* **14**, e1007050,
645 doi:10.1371/journal.ppat.1007050 (2018).

646 44 Lamiable, O. *et al.* Cytokine Dieldel and a viral homologue suppress the IMD
647 pathway in Drosophila. *Proceedings of the National Academy of Sciences of the*
648 *United States of America* **113**, 698-703, doi:10.1073/pnas.1516122113 (2016).

649 45 Ferreira, A. G. *et al.* The Toll-Dorsal Pathway Is Required for Resistance to Viral
650 Oral Infection in Drosophila. *Plos Pathogens* **10**, doi:ARTN e1004507
651 10.1371/journal.ppat.1004507 (2014).

652 46 Broderick, N. A., Buchon, N. & Lemaitre, B. Microbiota-induced changes in
653 drosophila melanogaster host gene expression and gut morphology. *mBio* **5**,
654 e01117-01114, doi:10.1128/mBio.01117-14 (2014).

655 47 Carpenter, J. *et al.* The transcriptional response of Drosophila melanogaster to
656 infection with the sigma virus (Rhabdoviridae). *PLoS One* **4**, e6838,
657 doi:10.1371/journal.pone.0006838 (2009).

658 48 West, C. & Silverman, N. p38b and JAK-STAT signaling protect against
659 Invertebrate iridescent virus 6 infection in Drosophila. *PLoS Pathog* **14**,
660 e1007020, doi:10.1371/journal.ppat.1007020 (2018).

661 49 Tanguy, M. *et al.* An Alternative STAT Signaling Pathway Acts in Viral Immunity
662 in Caenorhabditis elegans. *MBio* **8**, doi:10.1128/mBio.00924-17 (2017).

663 50 Lafont, M. *et al.* Long-lasting antiviral innate immune priming in the
664 Lophotrochozoan Pacific oyster, Crassostrea gigas. *Sci Rep* **7**, 13143,
665 doi:10.1038/s41598-017-13564-0 (2017).

666 51 Robalino, J. *et al.* Double-stranded RNA induces sequence-specific antiviral
667 silencing in addition to nonspecific immunity in a marine shrimp: convergence
668 of RNA interference and innate immunity in the invertebrate antiviral response?
669 *J Virol* **79**, 13561-13571, doi:10.1128/JVI.79.21.13561-13571.2005 (2005).

670 52 Lamiable, O. *et al.* Analysis of the Contribution of Hemocytes and Autophagy to
671 Drosophila Antiviral Immunity. *J Virol* **90**, 5415-5426, doi:10.1128/JVI.00238-16
672 (2016).

673 53 Sarov, M. *et al.* A genome-wide resource for the analysis of protein localisation
674 in Drosophila. *Elife* **5**, e12068, doi:10.7554/eLife.12068 (2016).

675 54 Yano, T. *et al.* Autophagic control of listeria through intracellular innate immune
676 recognition in drosophila. *Nature immunology* **9**, 908-916, doi:10.1038/ni.1634
677 (2008).

- 678 55 Holleufer, A. & Hartmann, R. A Highly Sensitive Anion Exchange
679 Chromatography Method for Measuring cGAS Activity in vitro. *Bio-protocol* **8**,
680 e3055, doi:10.21769/BioProtoc.3055 (2018).
- 681 56 Dobin, A. *et al.* STAR: ultrafast universal RNA-seq aligner. *Bioinformatics* **29**,
682 15-21, doi:10.1093/bioinformatics/bts635 (2013).
- 683 57 Liao, Y., Smyth, G. K. & Shi, W. featureCounts: an efficient general purpose
684 program for assigning sequence reads to genomic features. *Bioinformatics* **30**,
685 923-930, doi:10.1093/bioinformatics/btt656 (2014).
- 686 58 Love, M. I., Huber, W. & Anders, S. Moderated estimation of fold change and
687 dispersion for RNA-seq data with DESeq2. *Genome Biol* **15**, 550,
688 doi:10.1186/s13059-014-0550-8 (2014).
- 689 59 Imrichova, H., Hulselmans, G., Atak, Z. K., Potier, D. & Aerts, S. i-cisTarget
690 2015 update: generalized cis-regulatory enrichment analysis in human, mouse
691 and fly. *Nucleic Acids Res* **43**, W57-64, doi:10.1093/nar/gkv395 (2015).
- 692 60 Lestradet, M., Lee, K. Z. & Ferrandon, D. Drosophila as a model for intestinal
693 infections. *Methods Mol Biol* **1197**, 11-40, doi:10.1007/978-1-4939-1261-2_2
694 (2014).
- 695

696

697 **Acknowledgments:** We thank Darren J. Obbard (University of Edinburgh) for
698 providing the Kallithea virus and Luis Teixeira (Instituto Gulbenkian de Ciência) for
699 providing the isogenized *Relish* mutant flies and *w¹¹¹⁸* genetic background control.

700 **Funding:** This work was supported by the ERANET Infect-ERA program (ANR-14-
701 IFEC-0005), the Agence Nationale de la Recherche (ANR-17-CE15-0014), the
702 Investissement d'Avenir Programs (ANR-10-LABX-0036 and ANR-11-EQPX-0022),
703 the Chinese National Overseas Expertise Introduction Center for Discipline Innovation"
704 (Project "111" (D18010)), CNRS and INSERM. Further support was provided to R.H.
705 by the Novo Nordisk foundation grant NNF17OC0028184 and to D.C. by Natural
706 Science Foundation of Guangdong Province (grant: [2016A030310278](#)) and Science
707 and Technology Planning Project of Guangzhou (grant: [201707010030](#)). **Author**
708 **contributions:** H.C., A.H., B.S., J.S., A.L., J.H., and J.H. performed experiments;
709 N.E.M. performed bioinformatics analysis; D.C. H.H.G and T.P. provided critical

710 materials; H.C., A.H., J.T.M., R.H., N.E.M. and J.L.I. designed the experiments and
711 analyzed the data; H.C., R.H., N.E.M. and J.L.I. wrote the manuscript. **Competing**
712 **interests:** The authors declare no competing financial interests. **Data and materials**
713 **availability:** RNA-seq data for CDNs injected flies have been submitted to the GEO
714 database (Gene Expression Omnibus: <http://www.ncbi.nlm.nih.gov/geo/>) with the
715 accession number GSE140955. All other data needed to evaluate the conclusions in
716 the paper are present in the paper or the Supplementary Materials.
717

718 **FIGURE LEGENDS:**

719

720 **Figure 1**

721 2'3'-cGAMP injection induces a dynamic dSTING-Relish dependent transcriptional
722 response in *D. melanogaster*. Relative gene expression of the indicated dSTING-
723 regulated genes at 6h (**A-D**) and 24h (**E-H**) after injection of Tris and different CDNs in
724 *dSTING*^{Control} or *dSTING*^{Rxn} mutant flies. *dSTING* and *srg1-3* were significantly induced
725 in *dSTING*^{Control} flies 6 hours post injection (hpi) with c-di-AMP, c-di-AMP, 3'3'-cGAMP
726 and 2'3'-cGAMP ($|t| \geq 4.807$, $P < 0.001$ for all comparisons of Tris vs CDN injections).
727 c-di-GMP injection did not lead to significant changes in gene expression at any
728 timepoint ($|t| \leq 0.184$, $P \geq 0.184$ for all comparisons of Tris vs c-di-GMP injected flies).
729 *srg1-3* were never significantly induced in *dSTING*^{Rxn} mutants 24hpi ($|t| \leq 3.290$, $P \geq$
730 0.200 for all comparisons of Tris vs CDN injections). *dSTING* was induced in
731 *dSTING*^{Rxn} mutants ($|t| \geq 2.963$, $P \leq 0.017$, for all comparisons of Tris vs CDN injections,
732 excluding c-di-GMP), but the level of expression was always significantly lower than in
733 control flies ($|t| \geq 19.043$, $P < 0.001$ for all pairwise comparisons between control and
734 *dSTING*^{Rxn}). (**I-K**) Expression levels of *srg1-3* at different times post-injection with Tris,
735 cyclic-di-GMP or 2'3'-cGAMP. (**L-O**) Expression levels of *dSTING* and *srg1-3* 6h post-
736 injection with Tris, cyclic-di-GMP or 2'3'-cGAMP in control (*w*¹¹¹⁸) and *w*¹¹¹⁸;*Rel*^{E20} (*Rel*
737 ^{-/-}) mutant flies. *dSTING* expression after Tris injection was similar between control and
738 *Rel*^{-/-} flies ($|t| = 0.659$, $P = 0.515$). After 2'3'-cGAMP injection, induction folds of *dSTING*
739 and *srg1-3* were always significantly lower in Relish mutant than in control flies ($|t| \geq$
740 5.480 , $P \leq 0.001$ for all comparison of differences in *dSTING* and *srg1-3* levels between
741 Tris and 2'3'-cGAMP injected flies). Data are from two independent experiments. Each
29

742 point represents a pool of 6 flies. Expression levels are shown relative to the
743 housekeeping gene *RpL32* and are normalized by experiment. Boxplots represent the
744 median (horizontal line) and 1st/3rd quartiles, with whiskers extending to points within
745 1.5 times the interquartile range. * - $P \leq 0.05$, ** - $P \leq 0.01$, *** - $P \leq 0.001$, n.s. – $P >$
746 0.05. For panels a-k, comparisons are shown relative to Tris injection in a given
747 genotype or timepoint.

748

749

750 **Figure 2**

751 2'3'-cGAMP induces a strong transcriptional response in *D.melanogaster*. **(A)**
752 Expression profiles of *dSTING*^{Control} flies injected with Tris, 2'3'-cGAMP or c-di-GMP
753 (6, 12 and 24h post-injection). All differentially expressed genes (DEG) between 2',3'-
754 cGAMP- and Tris- injected flies for at least one timepoint or on average across all time
755 points are shown. Values are normalized to the mean log (expression) of Tris-injected
756 flies across the three time points. Expression profiles of stimulated and repressed
757 genes in 2'3'-cGAMP-injected flies were clustered by partition around medoids. **(B)**
758 Normalized mean gene expression by experimental condition in each temporal
759 expression profiles and across the different timepoints. **(C)** Expression of some
760 representative genes discussed in the text. **(D)** Gene ontology enrichment analysis of
761 the DEGs across the different temporal expression profiles. **BP**: Biological process,
762 **MF**: Molecular function, **CC**: Cellular compartment. Size and color of circles indicates
763 respectively the number of DEG and $-\log(P\text{-value})$ for the enrichment of each category.
764 **(E)** Numbers of DEGs potentially regulated by **Stimulated** transcription factors and

765 cytokines. Genes with high confidence binding sites for other TFs (**Call**) of the same
766 family are included.

767

768 **Figure 3**

769 2'3'-cGAMP injection induces a broad, dSTING-dependent, antiviral protection in *D.*
770 *melanogaster*. (**A-C**) Relative DCV (**A**) or CrPV (**B**) RNA loads and survival after
771 infection with DCV (**C**) of *dSTING^{Control}* and *dSTING^{Rxn}* mutant flies after co-injection of
772 virus and Tris, 2'3'-cGAMP or c-di-GMP at different days post-injection (d.p.i.). Co-
773 injection with 2'3'-cGAMP resulted in a significant decrease of viral RNA in
774 *dSTING^{Control}* flies 2 and 3 dpi ($|t| \geq 2.712$, $P \leq 0.020$ for Tris vs 2'3'-cGAMP
775 comparisons and $|t| \leq 0.112$, $P \geq 0.985$ for Tris vs c-di-GMP) but not in mutant flies ($|t|$
776 ≤ 1.547 , $P \geq 0.222$) and a significant increase in survival in control but not in mutant
777 flies ($z = 2.404$, $P = 0.032$ and $z = -0.433$, $P = 0.665$ for *dSTING^{Control}* and *dSTING^{Rxn}*
778 flies, respectively, for the pairwise comparisons between Tris and 2'3'-cGAMP after a
779 Cox proportional hazards model). (**D-F**) Relative viral loads at different time points of
780 control flies after co-injection of Tris, 2'3'-cGAMP or c-di-GMP with the viruses VSV
781 (**D**), FHV (**E**) or KV (**F**). Co-injection with 2'3'-cGAMP, but not c-di-GMP led to a
782 significantly reduced accumulation of all tested viruses ($|t| \geq 2.276$, $P \leq 0.049$ and $|t| \leq$
783 1.769 , $P \geq 0.148$ for all pairwise comparisons of Tris vs 2'3'-cGAMP or c-di-GMP at the
784 different days). Data are from two or three independent experiments. For panels a,b
785 and d-f, each point represents a pool of 6 flies. Expression levels are shown relative to
786 the housekeeping gene *RpL32* and are normalized by experiment. Boxplots represent
787 the median (horizontal line) and 1st/3rd quartiles, with whiskers extending to points
788 within 1.5 times the interquartile range. * - $P \leq 0.05$, ** - $P \leq 0.01$, *** - $P \leq 0.001$.

789

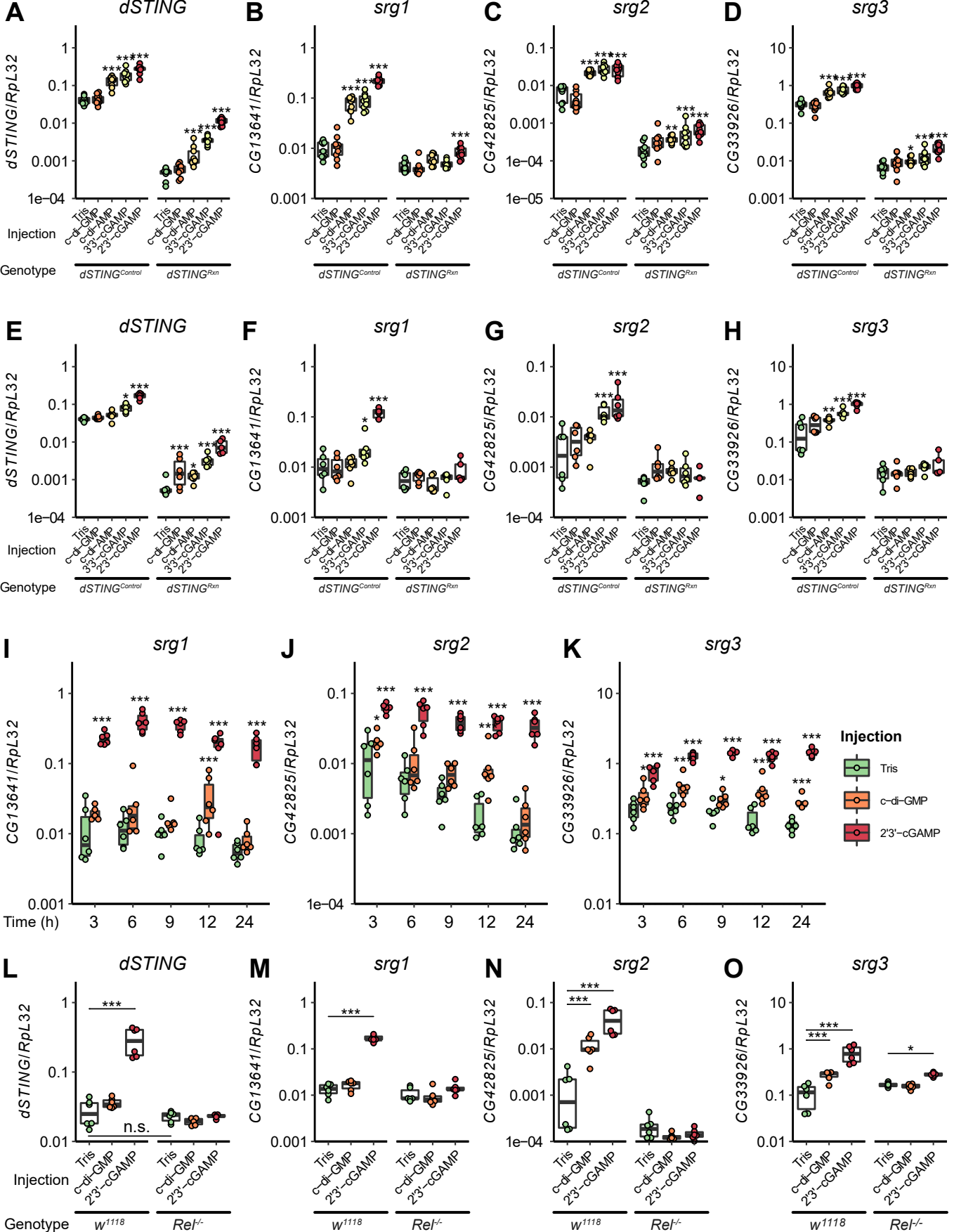
790 **Figure 4**

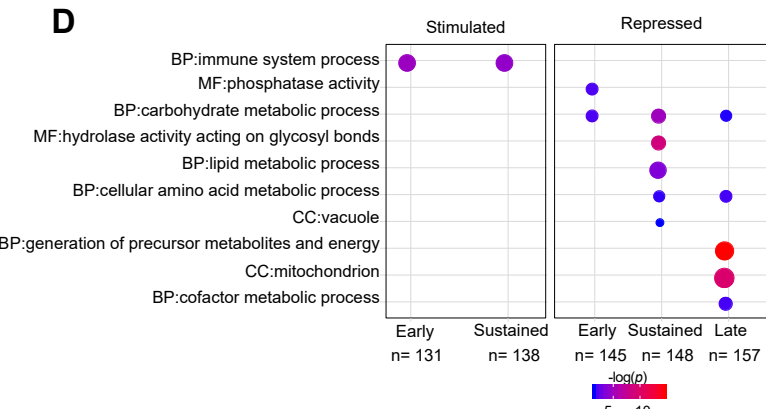
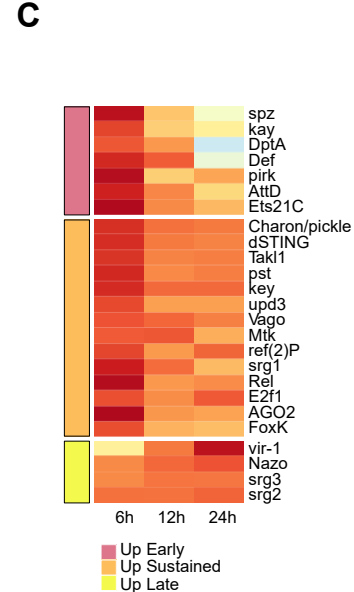
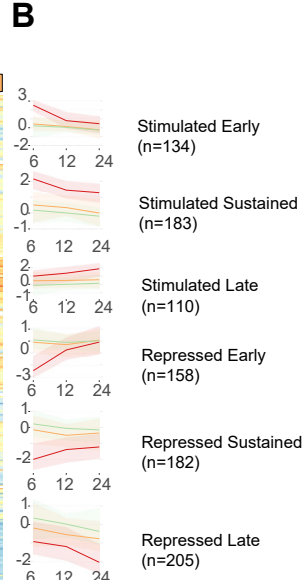
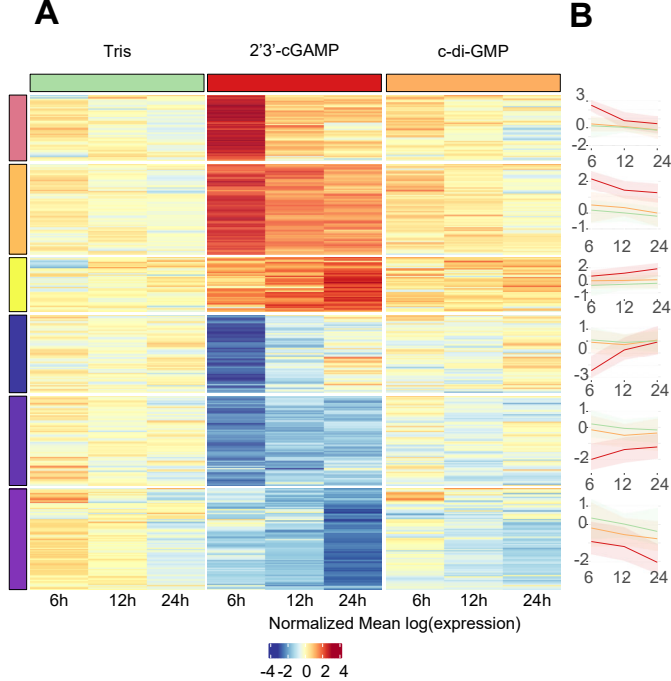
791 2'3'-cGAMP induced antiviral protection is dependent on Relish, but not on Atg7 or
792 AGO2. Viral RNA loads at different time points after co-injection of Tris or 2'3'-cGAMP
793 with DCV or VSV in flies mutant for the siRNA pathway (*yw;Ago2^{d414} - Ago2^{-/-}*, **A,B**),
794 autophagy (*Atg7^{d14/d77} - Atg7^{-/-}*, **C**), Relish (*w¹¹¹⁸;Rel^{E20} - Rel^{-/-}*, **D-F**), or in control flies
795 of the same genetic background (*yw, Atg7^{d14}/CG5335^{d30} - Atg7^{-/+}* or *w¹¹¹⁸*,
796 respectively). Co-injection with 2'3'-cGAMP led to a reduced accumulation of viral
797 RNAs in RNAi or autophagy impaired flies (Tris vs 2'3'-cGAMP comparisons, $|t| \geq 2.30$,
798 $P \leq 0.024$ across all timepoints) and in their controls ($|t| \geq 2.53$, $P \leq 0.013$ across all
799 timepoints) but not in Relish mutants ($|t| \leq 1.220$, $P \geq 0.225$ across all timepoints). Data
800 are from two or four (**D**) independent experiments. Each point represents a pool of 6
801 flies. Expression levels are shown relative to the housekeeping gene *RpL32* and are
802 normalized by experiment. Triangles indicate points where viral RNA could not be
803 detected: threshold cycles (Cq) values for these points were replaced by the maximum
804 Cq for a virus infected sample + 1. Boxplots represent the median (horizontal line) and
805 1st/3rd quartiles, with whiskers extending to points within 1.5 times the interquartile
806 range. * - $P \leq 0.05$, ** - $P \leq 0.01$, *** - $P \leq 0.001$.

807

808

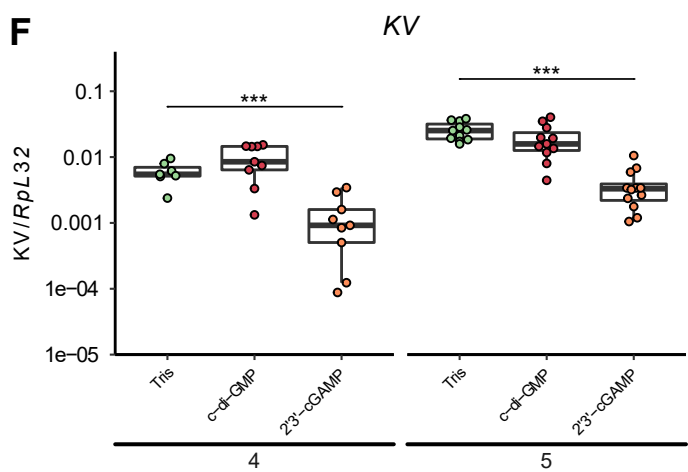
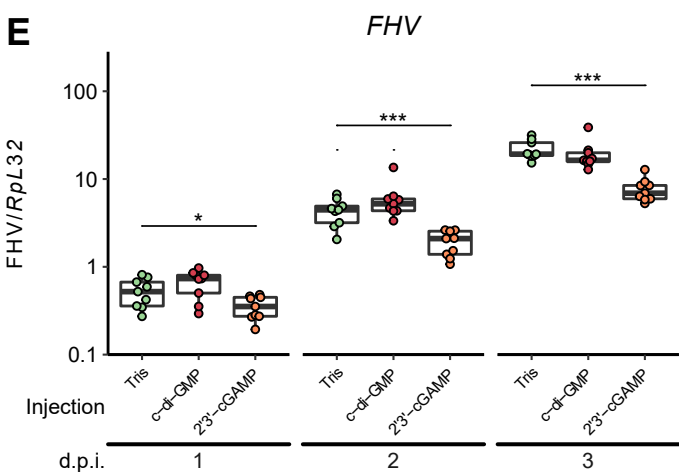
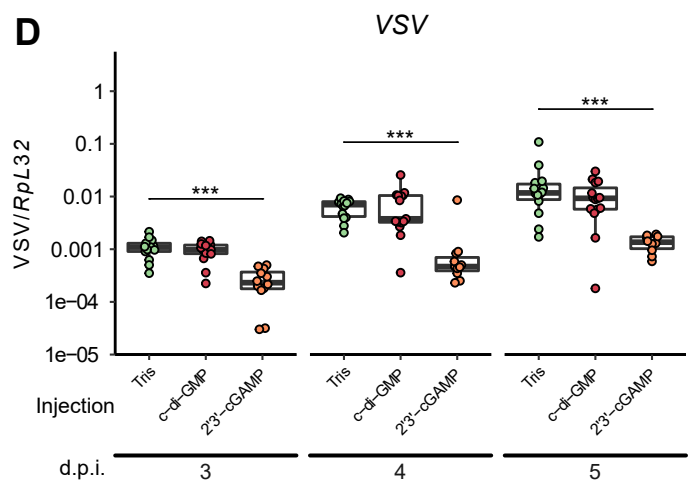
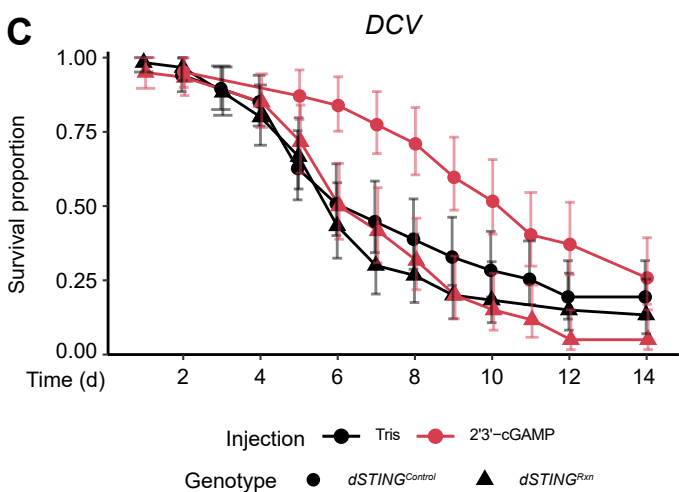
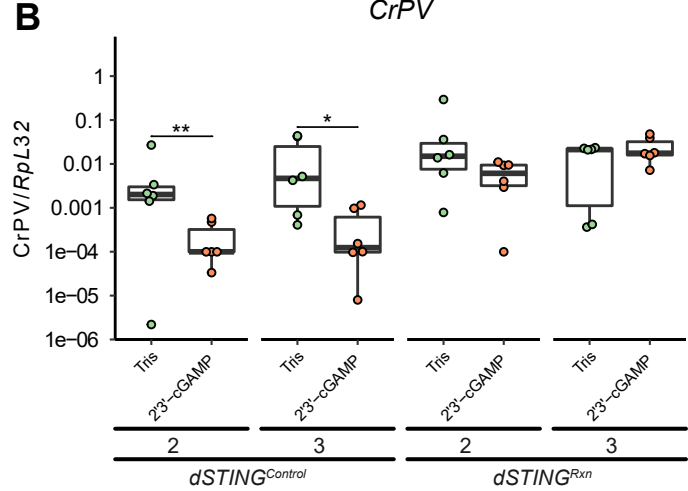
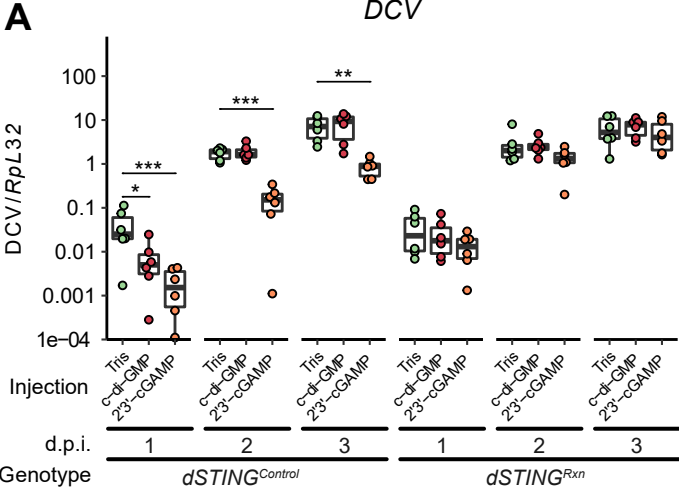
809 60

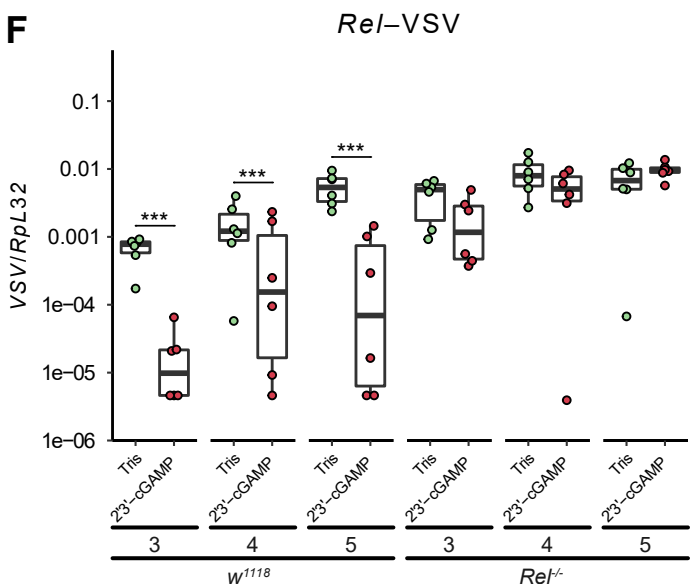
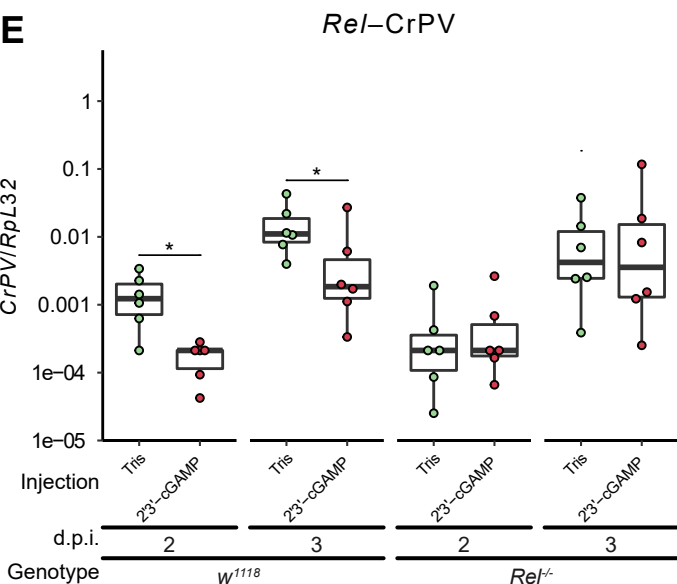
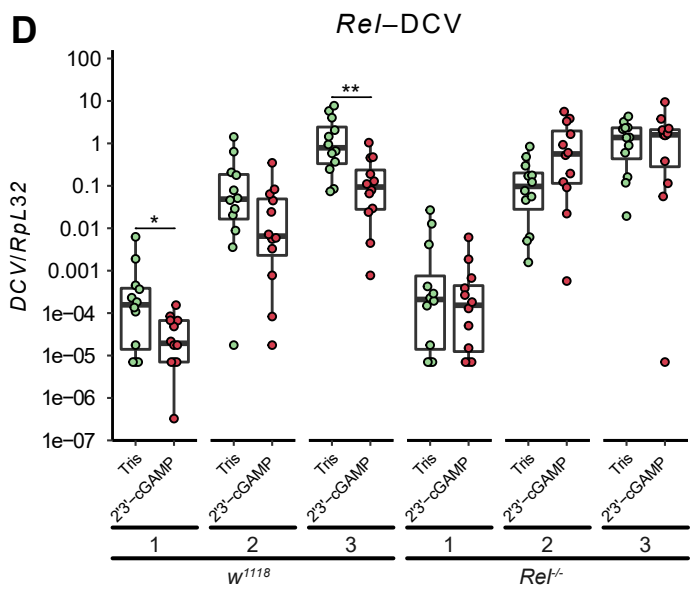
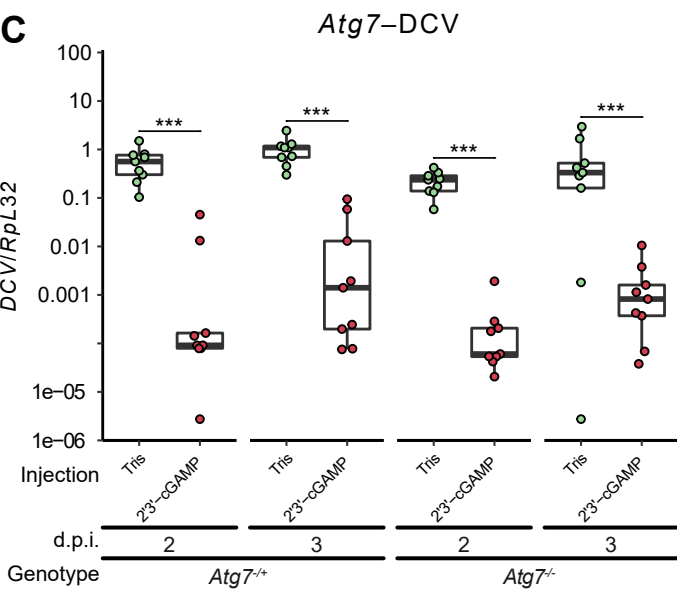
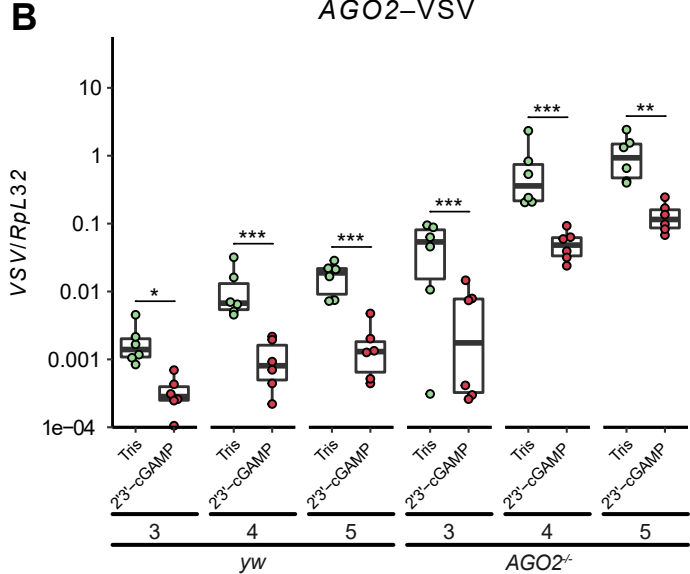
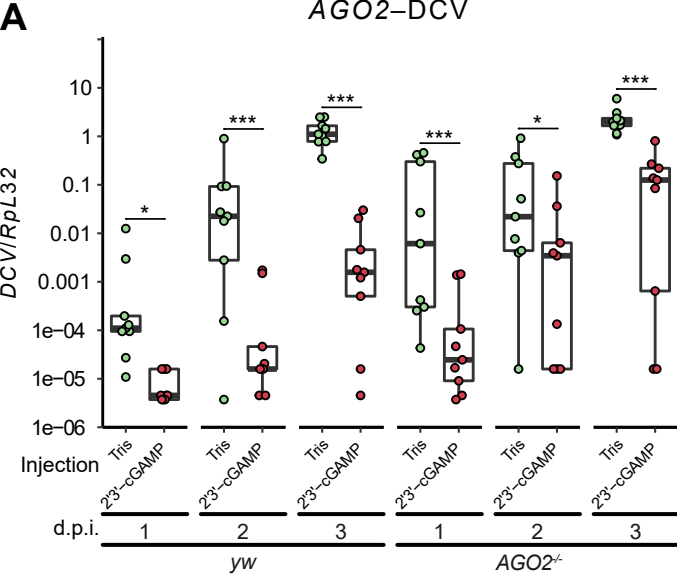




E

Family	Call	Stimulated	Stim. Early	Stim. Sustained	Stim. Late
NF- κ B	Dif, dl, Rel	Spz, Rel	112	146	63
AP-1	Jra, kay	kay	36	92	0
ETS	Ets97D, Ets98B, Eip74EF, Ets21C, Ets96B, pnt, aop	Ets21C, edl	31	0	0
STAT	Stat92E	upd3	29	77	9
E2F	E2f1	E2f1	23	0	0
Forkhead	Croc, fd59A, FoxP, CHES-1-like	FoxK	0	16	16
Hox/Hox-like	Ro, Ubx	Ubx	0	0	12





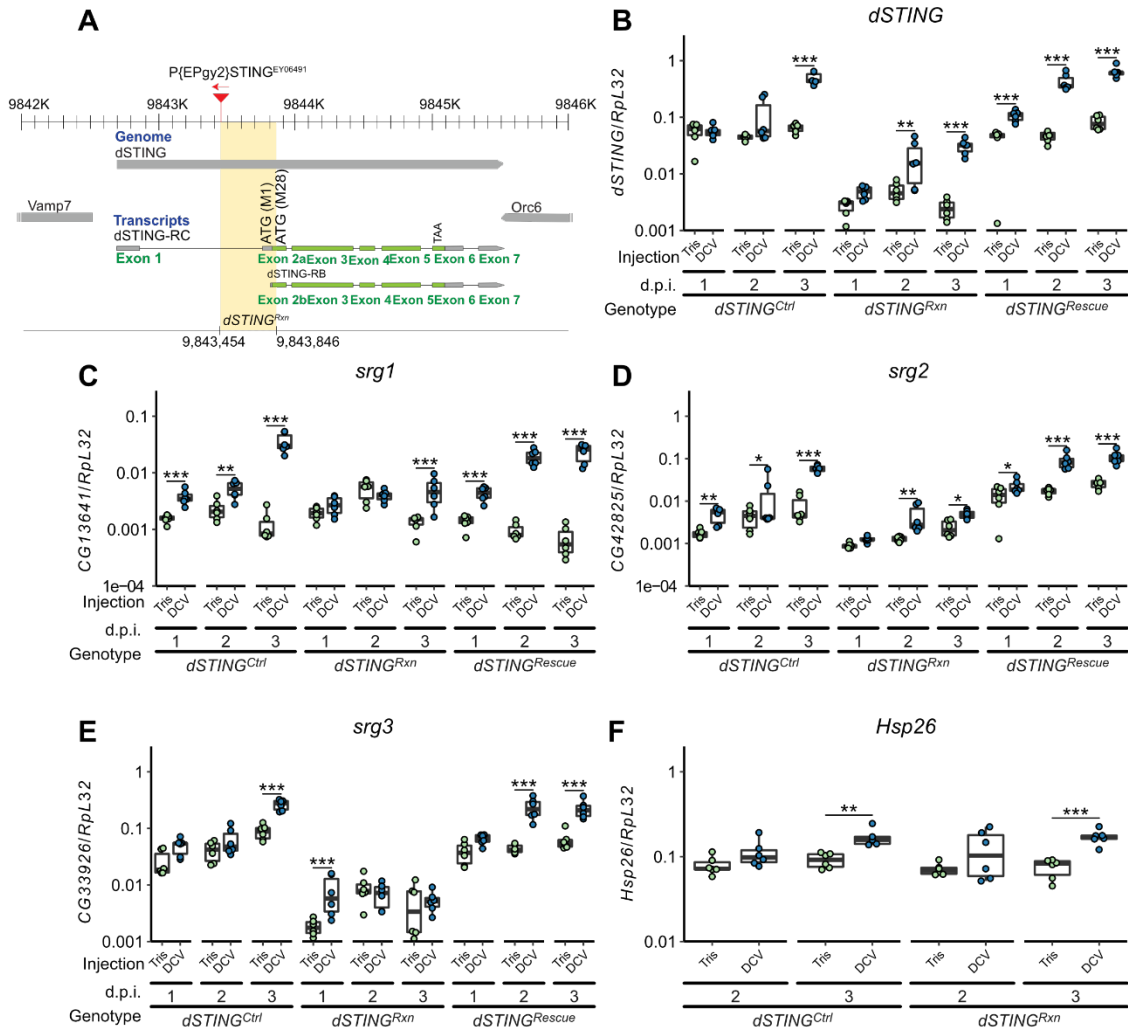


Figure S1 - DCV infection induces a dSTING dependent transcriptional response in *D. melanogaster*.

(A) *dSTING*^{Rxn} mutant flies were generated by imprecise excision of the P-element P{EPgy2}Sting^{EY06491}. The boundaries of the deletion (yellow shading), which removes the 3' end of the first intron and the 5' extremity of exons 2a and 2b of the two reported transcripts (RB and RC), are indicated at the bottom. Precise excision of the transposon generated control flies (*dSTING*^{Control}) in the same genetic background. (B-E) Relative gene expression at different days post-injection (d.p.i.) of Tris or DCV for *dSTING* (B) and *srg1-3* (C-E) in *dSTING*^{Control}, *dSTING*^{Rxn} mutant flies and *dSTING*^{Rxn} mutant flies containing a genomic

dSTING rescue transgene (*dSTING^{Rescue}*). Expression of *dSTING* was significantly lower in *dSTING^{Rxn}* mutant ($t \geq -7.189$, $P \leq 0.001$ in all pairwise comparisons between control and *dSTING^{Rxn}* in the different timepoints) and identical to control levels in rescue flies ($|t| \leq 2.044$, $P \geq 0.142$ in all pairwise comparisons between control and *dSTING^{Rescue}* in the different timepoints). *STING* is induced by DCV infection in *dSTING^{Rxn}* mutant flies ($|t| \geq 3.632$, $P \leq 0.001$ for all pairwise comparisons between Tris and DCV injected *dSTING^{Rxn}*) and reaches levels close to wild type three days post infection ($|t| = 2.466$, $P = 0.065$ for the comparison between DCV injected *dSTING^{Rxn}* and Tris injected control flies). Induction of *srg1* was lower at three dpi in *dSTING^{Rxn}* mutants, stimulation of *srg2* was lower at 3 dpi ($t = 0.6252$, $P = 0.002$) and levels of *srg3* were similar in Tris and DCV infected *dSTING^{Rxn}* mutants 2- and 3- dpi ($|t| \leq 1.268$, $P \geq 0.446$) and always lower than in control flies (> 4.85 fold, $|t| \geq 5.568$, $P < 0.001$). All these genes were induced by DCV infection in control or *dSTING^{Rescue}* flies two or three dpi ($|t| \geq 2.520$, $|P| \leq 0.037$), except for *srg3* in control flies 2 dpi ($t = 1.393$, $P = 0.373$) (F) Expression levels of *Hsp26*, a *dSTING*-independent virus induced gene. Induction of *Hsp26* by DCV was identical in control and *dSTING^{Rxn}* ($|t| \leq 0.842$, $P \geq 0.405$, comparison of differences in *Hsp26* levels between Tris and DCV injected flies at 2 or 3 d.p.i.). Data are from two independent experiments. Each point represents a pool of 6 flies. Expression levels are shown relative to the housekeeping gene *RpL32* and are normalized by experiment. Boxplots represent the median (horizontal line) and 1st/3rd quartiles, with whiskers extending to points within 1.5 times the interquartile range. * - $P \leq 0.05$, ** - $P \leq 0.01$, *** - $P \leq 0.001$.

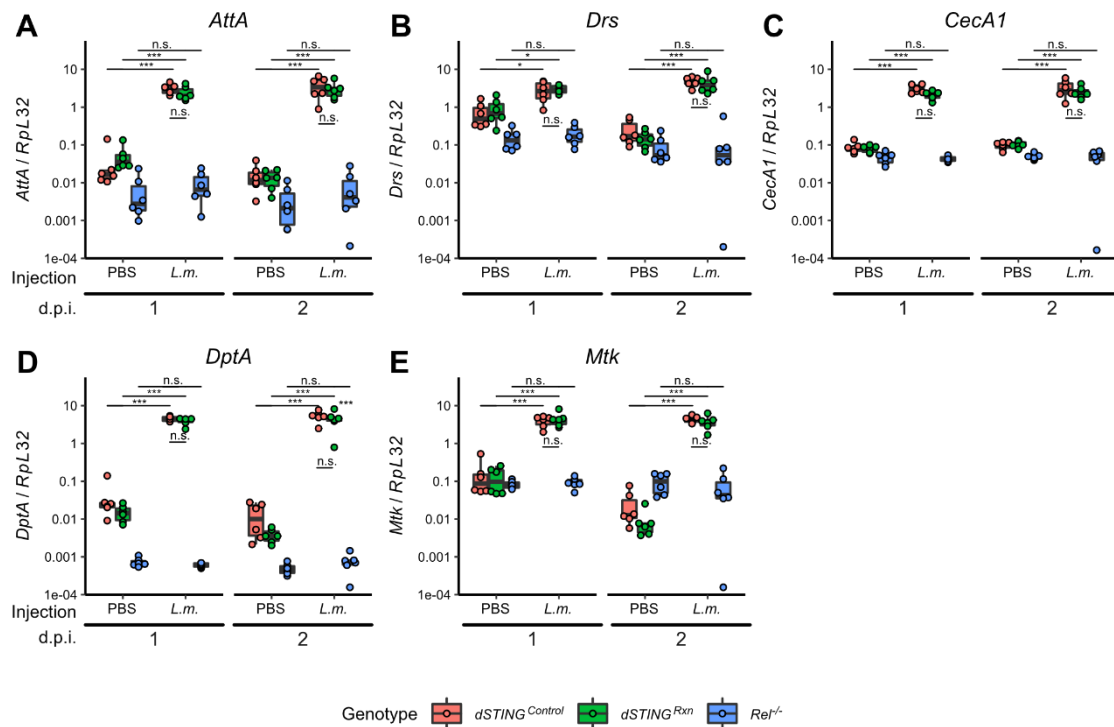


Figure S2 - Antimicrobial peptide gene induction is not affected in *dSTING* mutant flies after *L. monocytogenes* challenge.

(A-E) Relative expression of the indicated antimicrobial peptide (AMP) genes one and two days post-injection (d.p.i.) with buffer (PBS) or the gram-negative bacteria *Listeria monocytogenes* (*L.m.*) in control (*dSTING*^{Control}), *dSTING* (*dSTING*^{Rxn}) or Relish (*Rel*^{-/-}) mutant flies. *L. monocytogenes* infection led to a sustained induction of all tested AMPs in control and *dSTING* mutant flies but not in Relish mutants (*L. monocytogenes* vs. PBS injection, $|t| \geq 2.503$, $p \leq 0.047$ in control or *dSTING* mutants and $|t| \leq 2.241$, $P \geq 0.076$ in *Rel*^{-/-} mutants). Expression levels were similar between control and *dSTING* mutants (control vs. *dSTING* mutants; $|t| \leq 1.911$, $P \geq 0.153$ for all comparisons except for *DptA* 1 d.p.i. after PBS injection $|t| = 2.689$, $P = 0.037$). Data are from two independent experiments. Each point represents a pool of 6 flies. Expression levels are shown relative to the housekeeping gene *RpL32* and are normalized by experiment.

Boxplots represent the median (horizontal line) and 1st/3rd quartiles, with whiskers extending to points within 1.5 times the interquartile range. * - $P \leq 0.05$, ** - $P \leq 0.01$, *** - $P \leq 0.001$, n.s. – $P > 0.05$.

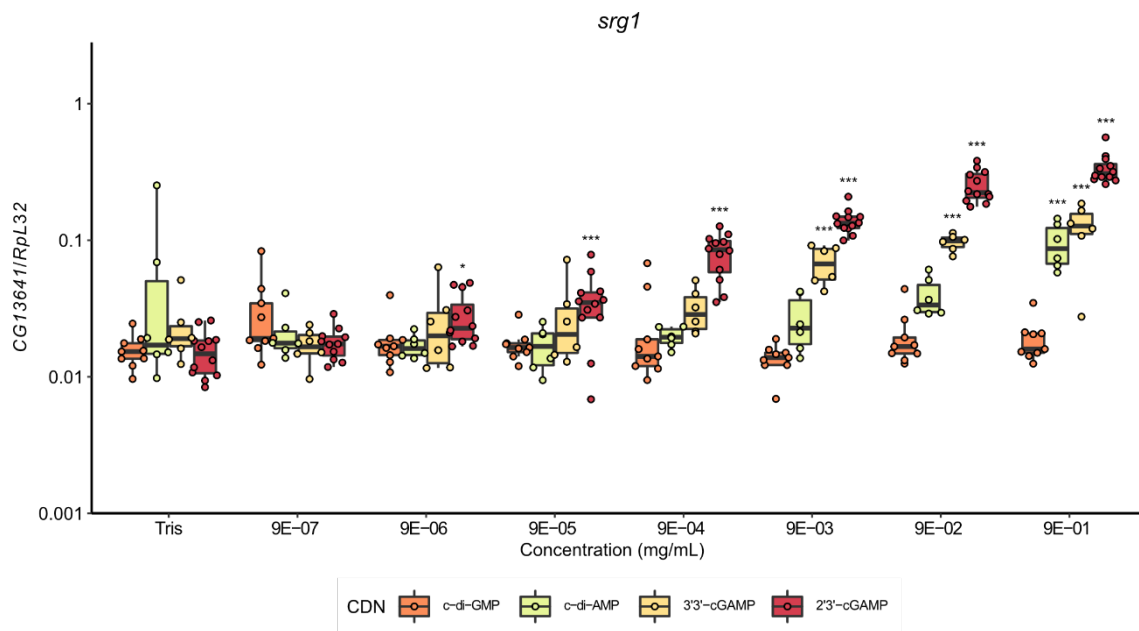


Figure S3 - The cyclic dinucleotides 2'3'-cGAMP, 3'3'-cGAMP and c-di-AMP have a dose dependent effect on the expression of a *dSTING* regulated gene. Relative expression of *srg1* six hours post-injection of buffer (Tris) and the cyclic dinucleotides (CDN) c-di-GMP, c-di-AMP, 3'3'-cGAMP and 2'3'-cGAMP in the indicated concentrations in control flies. *srg1* was induced after injection with concentrations above 9×10^{-6} mg/mL of 2'3'-cGAMP (CDN vs matched Tris comparison, $|t| \geq 3.177$, $P \leq 0.011$), 9×10^{-3} of 3'3'-cGAMP ($|t| \geq 4.358$, $P < 0.001$) and 0.9 of c-di-AMP ($|t| \geq 4.281$, $P < 0.001$). Injection of c-di-GMP at any concentration did not lead to changes in *srg1* expression ($|t| \leq 2.476$, $P \geq 0.078$). Data are from four (2'3'-cGAMP), three (c-di-GMP) or two independent experiments (3'3'-cGAMP and c-di-AMP). Each point represents a pool of 6 flies. Expression levels are shown relative to the housekeeping gene *RpL32* and are normalized by experiment. Boxplots represent the median (horizontal line) and 1st/3rd quartiles, with whiskers extending to points within 1.5 times the

interquartile range. * - $P \leq 0.05$, ** - $P \leq 0.01$, *** - $P \leq 0.001$. Comparisons are shown relative to the matched Tris injection for a given CDN.

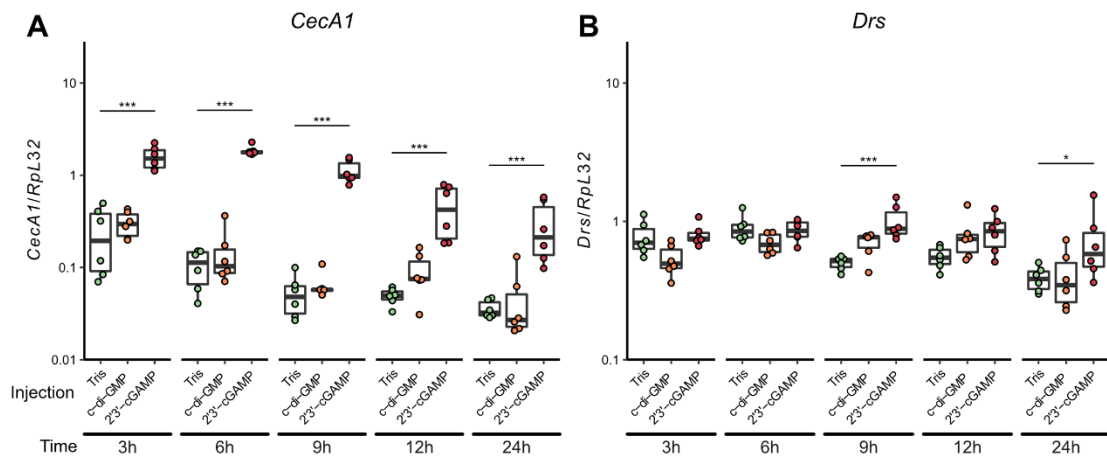


Figure S4 - c-di-GMP injection does not induce antimicrobial peptide expression.

(A-B) Relative expression of the indicated antimicrobial peptides in control flies across time (h). *CecA1* was sustainedly induced after six or three hours post-injection with 2'3'-cGAMP ($|t| \geq 6.152$, $P < 0.001$) but not after injection with c-di-GMP ($|t| \leq 2.506$, $|P| \geq 0.072$). Data are from two independent experiments. Each point represents a pool of 6 flies. Expression levels are shown relative to the housekeeping gene *RpL32* and are normalized by experiment. Boxplots represent the median (horizontal line) and 1st/3rd quartiles, with whiskers extending to points within 1.5 times the interquartile range. * - $P \leq 0.05$, ** - $P \leq 0.01$, *** - $P \leq 0.001$.

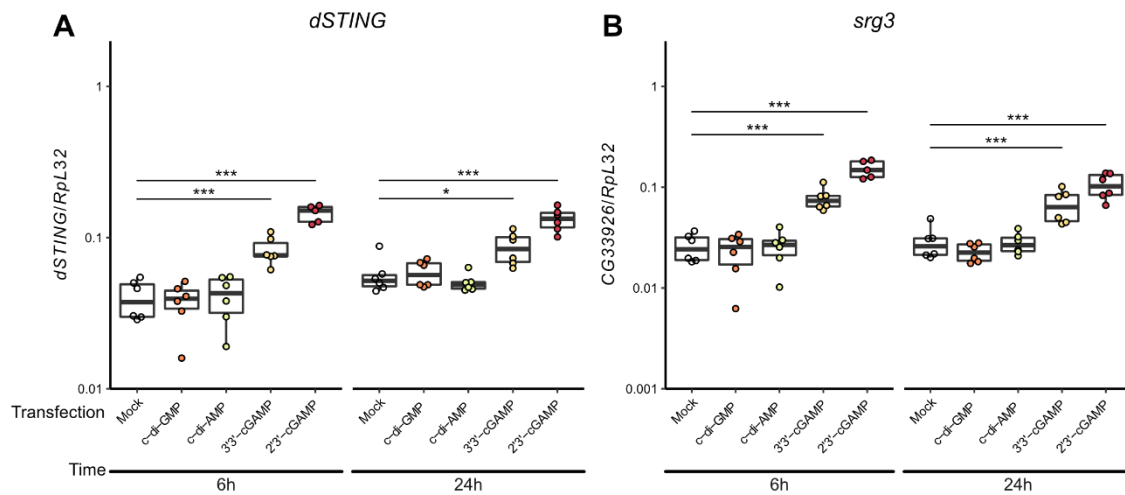


Figure S5 – The cyclic dinucleotides 2'3'-cGAMP and 3'3'-cGAMP induce *dSTING* dependent genes in a cellular model.

Relative expression of *dSTING* (**A**) and *srg3* (**B**) six and 24 hours post-transfection with Effectene transfection reagent (Mock) and the cyclic dinucleotides (CDN) c-di-GMP, c-di-AMP, 3'3'-cGAMP and 2'3'-cGAMP in drosophila S2 cells. *dSTING* and *srg3* were induced six and 24 hours after transfection with 2'3'-cGAMP and 3'3'-cGAMP (CDN vs Mock $|t| \geq 2.702$, $P < 0.034$). Transfection of c-di-AMP or c-di-GMP at any concentration did not lead to changes in gene expression ($|t| \leq 1.022$, $P \geq 0.673$). Data are from two independent experiments. Each point represents an independent pool of cells. Expression levels are shown relative to the housekeeping gene *RpL32*. Boxplots represent the median (horizontal line) and 1st/3rd quartiles, with whiskers extending to points within 1.5 times the interquartile range. * - $P \leq 0.05$, ** - $P \leq 0.01$, *** - $P \leq 0.001$.

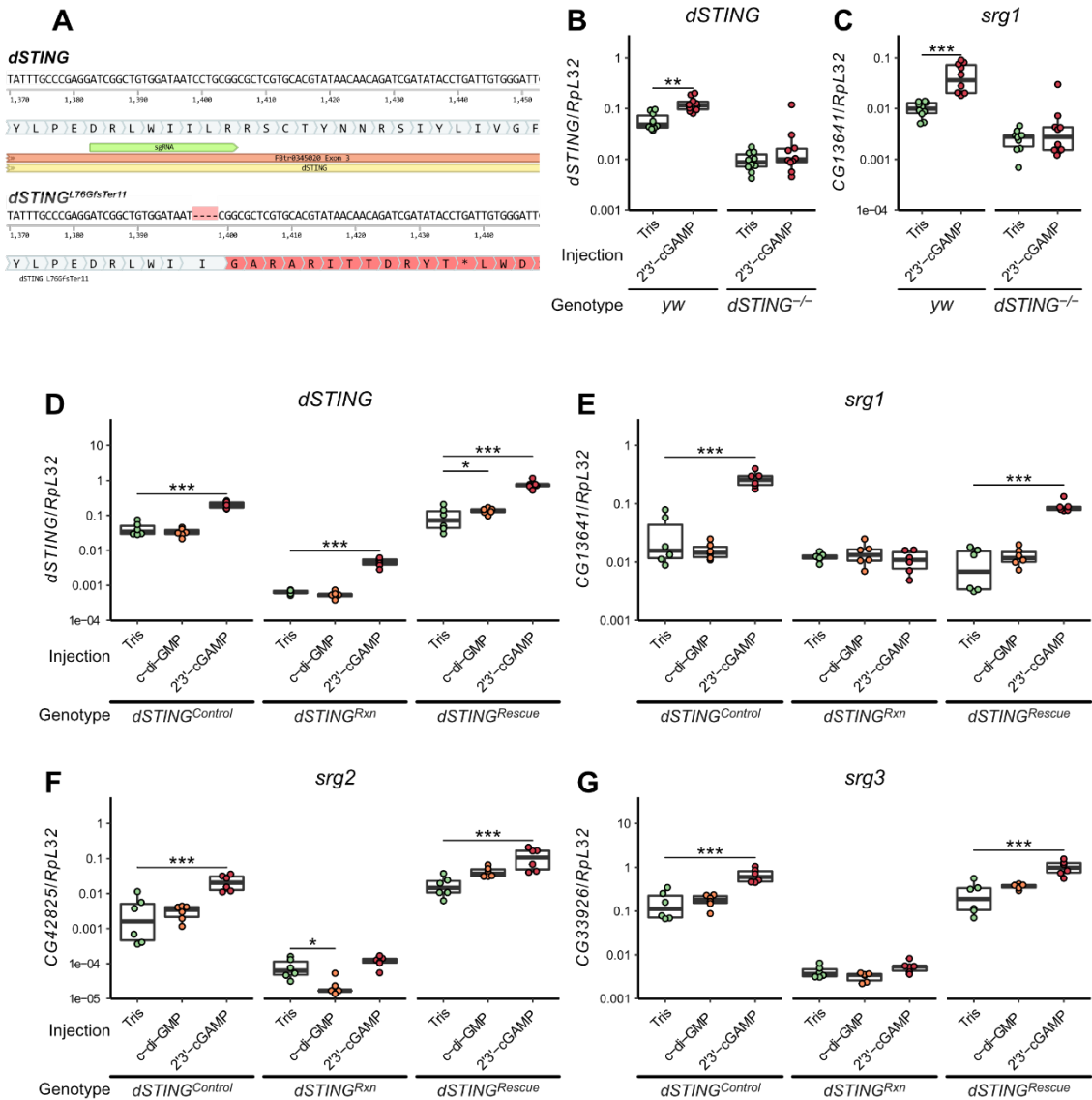


Figure S6 – Induction of gene expression following 2'3'-cGAMP injection depends on dSTING.

(A) Sequence of wild-type *dSTING* (top) and *dSTING^{L76GfsTer11}* (bottom) in the vicinity of the sgRNA targeted region (sg). Open reading frame translations are shown below the sequences. Coordinates are in nucleotides, relative to the gene start. (B,C) Relative expression of the indicated dSTING-regulated genes at 6h after injection of buffer (Tris) or 2'3'-cGAMP in control (*yw*) or *yw;dSTING^{L76GfsTer11}* (*dSTING^{-/-}*) mutant flies. (D-G) Relative expression of the indicated dSTING-regulated genes at 6h after injection of buffer (Tris) or 2'3'-cGAMP in control (*dSTING^{Control}*), *dSTING* mutants (*dSTING^{Rxn}*) and *dSTING*

mutants complemented by a genomic rescue of *dSTING* (FlyFos015653;*dSTING^{Rescue}*). *dSTING* and *srg1* were induced by 2'3'cGAMP injection in *yw* flies ($|t| \geq 3.009$, $p \leq 0.01$) but not in *dSTING^{-/-}* mutants ($|t| \leq 1.561$, $p \geq 0.128$). *srg1-3* were induced after 2'3'cGAMP injection in control and *dSTING^{Rescue}* flies but not in *dSTING^{Rxn}* mutant flies (Tris vs. 2'3'cGAMP injections, $|t| \geq 4.359$, $p < 0.001$ in control or *dSTING^{Rescue}* flies and $|t| \leq 1.102$, $p \geq 0.718$ in *dSTING^{Rxn}*); *dSTING* was induced by 2'3'cGAMP injection in all genotypes ($|t| \geq 7.925$, $p < 0.001$). Data are from three (a-b) or two (c-f) independent experiments. Each point represents a pool of 6 flies. Expression levels are shown relative to the housekeeping gene *RpL32* and are normalized by experiment. Boxplots represent the median (horizontal line) and 1st/3rd quartiles, with whiskers extending to points within 1.5 times the interquartile range. * - $p \leq 0.05$, ** - $p \leq 0.01$, *** - $p \leq 0.001$.

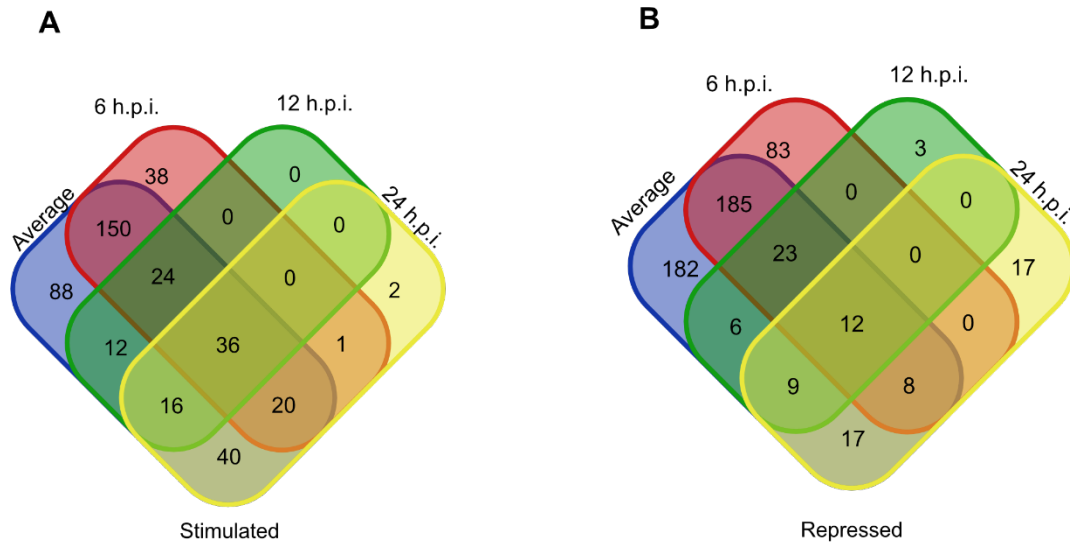


Figure S7 - Differentially expressed transcripts between Tris and 2'3'-cGAMP injected flies in the different timepoints.

Venn diagram of the **(A)** stimulated and **(B)** repressed genes between 2'3'-cGAMP and Tris injected *dSTING^{Control}* flies at the different timepoints (6, 12 and 24h) after injection or on average across all timepoints.

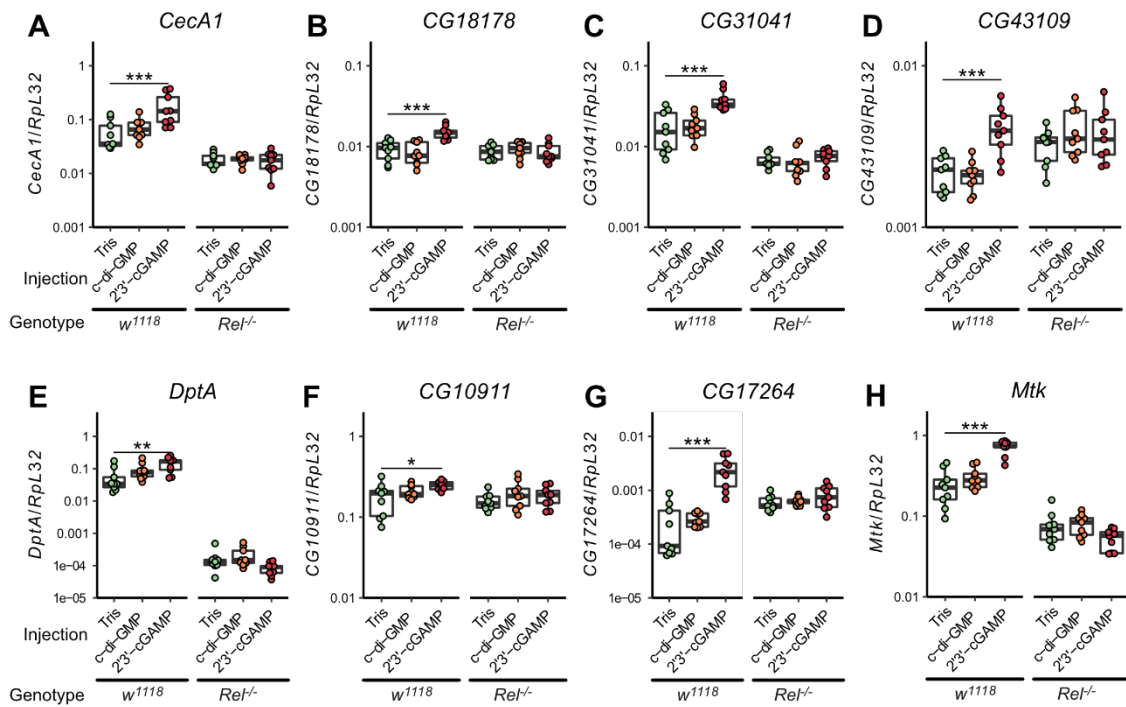


Figure S8 - 2'3'-cGAMP induced gene expression is *Relish* dependent.

Relative expression of the indicated genes six hours post-injection of buffer (Tris), c-di-GMP or 2'3'-cGAMP in control (*w¹¹¹⁸*) or *Relish* (*Rel^{-/-}*) mutant flies. Genes classified as early (A-E) or sustained (F-H) induced by 2'3'-cGAMP injection according to the RNAseq analysis were induced by 2'3'-cGAMP in control (2'3'-cGAMP vs Tris comparisons, $|t| \geq 2.781$, $P \leq 0.031$) but not in *Rel^{-/-}* mutants ($|t| \leq 1.932$, $P \geq 0.178$). c-di-GMP injection did not lead to changes in expression of any of the tested genes ($|t| \leq 2.180$, $P \geq 0.102$). Data are from three independent experiments. Each point represents a pool of 6 flies. Expression levels are shown relative to the housekeeping gene *RpL32* and are normalized by experiment. Boxplots represent the median (horizontal line) and 1st/3rd quartiles, with whiskers extending to points within 1.5 times the interquartile range. * - $P \leq 0.05$, ** - $P \leq 0.01$, *** - $P \leq 0.001$.

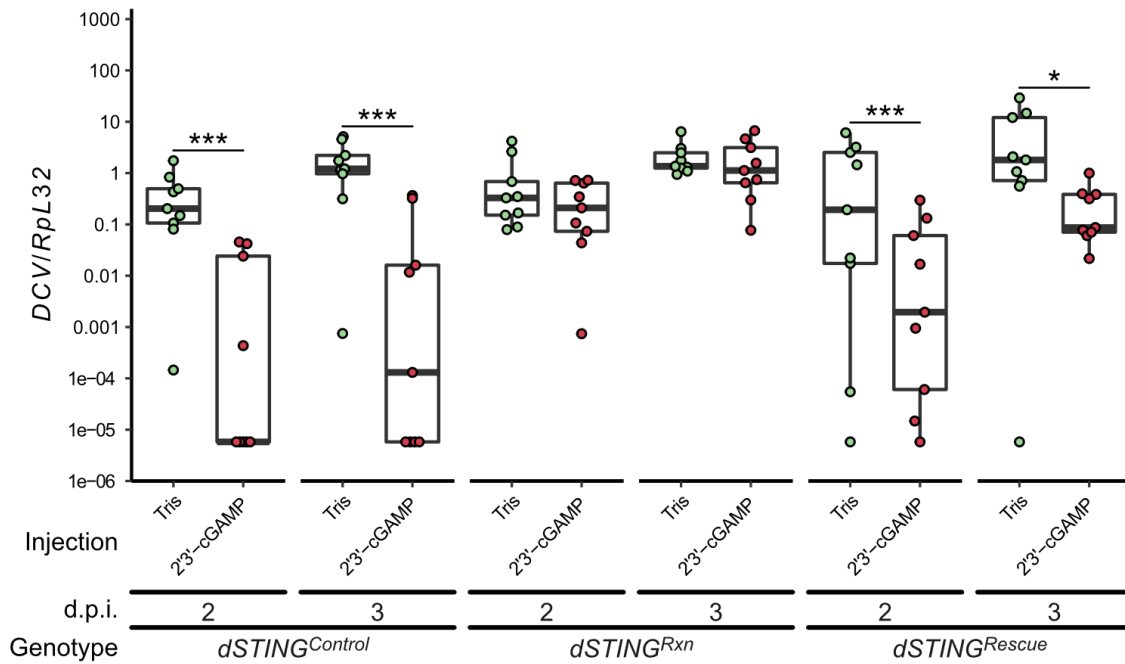


Figure S9 - A *dSTING* rescue transgene restores 2'3'-cGAMP induced antiviral protection.

Relative load of DCV RNA at 2 and 3 days after co-injection (d.p.i.) with buffer (Tris), c-di-GMP or 2'3'-cGAMP in control (*dSTING^{Control}*), *dSTING* mutants (*dSTING^{Rxn}*) and *dSTING* mutants complemented by a genomic rescue of *dSTING* (FlyFos015653;*dSTING^{Rescue}*). DCV RNA loads were lower after co-injection with 2'3'-cGAMP in control and *dSTING^{Rescue}* flies but not in *dSTING^{Rxn}* mutants (Tris vs 2'3'-cGAMP injections, $|t| \geq 2.724$, $P \leq 0.019$ in control or *dSTING^{Rescue}* flies and $|t| \leq 0.693$, $P \geq 0.976$ in *dSTING^{Rxn}*). Data are from three independent experiments. Each point represents a pool of 6 flies. Expression levels are shown relative to the housekeeping gene *RpL32* and are normalized by experiment. Boxplots represent the median (horizontal line) and 1st/3rd quartiles, with whiskers extending to points within 1.5 times the interquartile range. * - $p \leq 0.05$, ** - $p \leq 0.01$, *** - $p \leq 0.001$.

Table S1 - List of used oligonucleotide primers.

Target	FlyBase ID	Forward Primer	Reverse Primer	Reference
qRT-PCR				
<i>RpL32</i>	FBgn0002626	GCCGCTTCAAGGGACAGTATCT	AAACGCGGTTCTGCATGAG	4
<i>AttA</i>	FBgn0012042	GGCCCATGCCAATTTATTC	AGCAAAGACCTTGGCATCC	4
<i>CecA1</i>	FBgn0000276	ACGCGTTGGTCAGCACACT	ACATTGGCGGCTTGTGAG	4
<i>CG13641</i>	FBgn0039239	GTGTCCATTATCCGCACAAG	ACTGGGTATCTGACGGATG	4
<i>dSTING</i>	FBgn0033453	CCGGTGTCTATCGTCCTTTC	CGCTTTAGTTCCTGCATCTG	4
<i>CG42825</i>	FBgn0262007	GCGTTTTGGCCCTTATTATG	CTTTTGTAGCCGACGCAGTG	4
<i>CG33926</i>	FBgn0053926	GCGACCGTCATTGGATTGG	TGATGGTCCCGTTGATAGCC	4
<i>Hsp26</i>	FBgn0001225	CTACAAGGTTCCCGATGGC	GAATACTGACGGTGAGCAG	This work
<i>DCV</i>		TCATCGGTATGCACATTGCT	CGCATAACCATGCTCTTCTG	4
<i>CrPV</i>		GCTGAAACGTTCAACGCATA	CCACTTGCTCCATTTGGTTT	4
<i>FHV</i>		TTTAGAGCACATGCGTCCAG	CGCTCACTTTCTTCGGGTTA	4
<i>KV</i>		CATCAATATCGCGCCATGCC	GACCGAGTTAGCGTCAATGC	4
<i>VSV</i>		CATGATCCTGCTCTTCGTCA	TGCAAGCCCGGTATCTTATC	4
<i>Drs</i>	FBgn0283461	CGTGAGAACCTTTTCCAATATGATG	TCCCAGGACCACCAGCAT	60
<i>DptA</i>	FBgn0004240	GCTGCGCAATCGTTCTACT	TGGTGGAGTGGGCTTCATG	60
<i>Mtk</i>	FBgn0014865	CGTCAACCAGGGACCCATTT	CCGGTCTTGGTTGGTTAGGA	60
<i>CG18178</i>	FBgn0036035	CGAAGACGAAGATTCCGATGG	TTGGGCTGCGTTTGATTGTA	This work; https://www.flyrnai.org/flyprimerbank
<i>CG31041</i>	FBgn0051041	ACGTGCAATGCGTGGACTAC	CCGTCGTAATTGTCCTTGAC	This work; https://www.flyrnai.org/flyprimerbank
<i>CG43109</i>	FBgn0262569	CTCATCCAAGGGCGTTCTGT	TCCCAGGGTGATGATCCCTT	This work; https://www.flyrnai.org/flyprimerbank
<i>CG10911</i>	FBgn0034295	TCCGCCCTGCAACTTAGTA	TCAAGGGTATGTCACCATCG	This work; https://www.flyrnai.org/flyprimerbank
<i>CG17264</i>	FBgn0031490	CGTTGCAGGAAATCTCTGATCG	GGGAACAGGGAACAGATGGATAA	This work; https://www.flyrnai.org/flyprimerbank
Sequencing				
dSTING	FBgn0033453	CACCTCTATTCGATTGTAGC	AGCCGTGAAAGTAGTTGGAG	This work

References - 60

Data S1 - Differentially expressed genes between Tris and c-di-GMP injected *dSTING^{Control}* flies at 6, 12 and 24 hours post-injection.

Columns represent Ensembl gene ID (**gene_id**) and symbol (**gene_symbol**), mean normalized counts after Tris (**TRIS_**) or c-di-GMP injection (**c-di-GMP_**) at the different timepoints (**_06,_12** or **_24**), together with estimated \log_2 (fold-change) (**lfc_**) and Benjamini-Hochberg corrected P-values for the comparison between c-di-GMP and Tris injected flies at each individual timepoint and on average across all timepoints (**_AVG**).

Data S2 - Differentially expressed genes between Tris and 2'3'-cGAMP injected *dSTING^{Control}* flies at 6, 12 and 24 hours post-injection.

Columns represent Ensembl gene ID (**gene_id**) and symbol (**gene_symbol**), temporal expression category (**category**) mean normalized counts after Tris (**TRIS_**) or 2'3'-cGAMP injection (**cGAMP_**) at the different timepoints (**_06,_12** or **_24**), together with estimated \log_2 (fold-change) (**lfc_**) and Benjamini-Hochberg corrected P-values for the comparison between c-di-GMP and Tris injected flies at each individual timepoint and on average across all timepoints (**_AVG**).

Data S3 - Differentially expressed transcription factors or cytokines between Tris and 2'3'-cGAMP injected *dSTING^{Control}* flies at 6, 12 and 24 hours post-injection.

Columns headings are as in data S2, and include the transcription factor family/sub-family (**Family**).

Data S4 - Presence of binding sites for stimulated transcription factors in differentially expressed genes.

Differentially expressed genes between Tris and 2'3'-cGAMP injected *dSTING*^{Control} flies with regulatory sequences enriched for the differentially expressed transcription factors, or for transcription factors of the same family/sub-family. Columns headings are as in data S3, and include the high confidence transcription factor calls predicted by RcisTarget.